Short title: Leaf oil production rearranges membrane lipid flux

Corresponding author: Philip D. Bates

Title: Reorganization of acyl flux through the lipid metabolic network in oil-accumulating tobacco leaves

Xue-Rong Zhou[1], Sajina Bhandari[2], Brandon S. Johnson[2], Hari Kiran Kotapati[2], Doug K. Allen[3], Thomas Vanhercke[1], Philip D. Bates[2]

1. CSRIO Agriculture & Food, Canberra, ACT, Australia
2. Washington State University, Pullman, WA, USA
3. United States Department of Agriculture-Agricultural Research Service, Donald Danforth Plant Science Center, St. Louis, MO, USA

One-sentence Summary:

Engineering leaves to accumulate oils induced unexpected changes to fatty acid flux through the leaf lipid metabolic network.

Footnotes:

Author contributions:

X.Z., T.V., and P.D.B. conceived the original research plans; X.Z., S.B., B.S.J., H.K., and P.D.B performed the experiments and analyzed the data; D.K.A, analyzed the data and contributed to the scope; P.D.B. wrote the article with contributions of all the authors; P.D.B. agrees to serve as the author responsible for contact and ensures communication.

Funding information:

This work is supported by Agriculture and Food Research Initiative Grant No. 2017-67013-26156, No. 2017-67013-29481, and the Hatch umbrella project #1015621 from

the USDA National Institute of Food and Agriculture, and the National Science Foundation Grant No. 1930559.

Author of Contact: phil_bates@wsu.edu

Abstract:

The triacylglycerols (TAGs; i.e., oils) that accumulate in plants represent the most energy dense form of biological carbon storage, and are used for food, fuels, and chemicals. The increasing human population and decreasing amount of arable land have amplified the need to produce plant oil more efficiently. Engineering plants to accumulate oils in vegetative tissues is a novel strategy, because most plants only accumulate large amounts of lipids in the seeds. Recently, tobacco (*Nicotiana tabacum*) leaves were engineered to accumulate oil at 15% of dry weight due to a push (increased fatty acid synthesis) and pull (increased final step of TAG biosynthesis) engineering strategy. However, to accumulate both TAG and essential membrane lipids, fatty acid flux through non-engineered reactions of the endogenous metabolic network must also adapt, which is not evident from total oil analysis. To increase our understanding of endogenous leaf lipid metabolism and its ability to adapt to metabolic engineering, we utilized a series of *in vitro* and *in vivo* experiments to characterize the path of acyl flux in wild-type and transgenic oil-accumulating tobacco leaves. Acyl flux around the phosphatidylcholine acyl editing cycle was the largest acyl flux reaction in wild-type and engineered tobacco leaves. In oil-accumulating leaves, acyl flux into the eukaryotic pathway of glycerolipid assembly was enhanced at the expense of the prokaryotic pathway. However, a direct Kennedy pathway of TAG biosynthesis was not detected as acyl flux through phosphatidylcholine preceded the incorporation into TAG. These results provide insight into the plasticity and control of acyl lipid metabolism in leaves.

Introduction

A finite supply of petroleum and a growing demand for energy to support increasingly industrialized nations are global factors that emphasize the vital need to

develop renewable and sustainable sources of energy dense liquid fuels. The demand is further exacerbated by growing populations and concerns linked to fossil fuel use and associated waste streams. Seed-derived vegetative oil, mainly consisting of triacylglycerol (TAG), provides a sustainable alternative. TAG-based plant oils are one of the most energy-dense compounds found in nature. Plant oils are predominantly used in the food industry (~80%), with the remainder supplying oleochemical production (Carlsson et al., 2011). Due to their high energy density, they are increasingly viewed as an attractive feed stock for production of biofuels (Lu et al., 2011). Breeding programs and crop research in the last half century have substantially raised yields of oilseed production, taking advantage of improved land, nutrient management, and more efficient farming practices. Nevertheless, further gains in yield will require innovative, if not disruptive, scientific approaches. The amount of arable land is finite and decreasing with urban sprawl. As the world population continues to grow, agriculture production must do more with less to meet food and energy demands. Non-seed derived plant oils which can accumulate more lipids per acre of land are an attractive strategy, including the production of oils in vegetative tissues of high biomass crops (Vanhercke et al., 2019).

Attempts to engineer oil in non-seed tissues have demonstrated increased TAG levels by targeting different aspects of lipid biosynthesis, storage, and protection. These include leaf, stem, tuber, root, or various vegetative tissues, in multiple plant species including: Arabidopsis (*Arabidopsis thaliana*), tobacco (*Nicotiana tabacum*), potato (*Solanum tuberosum*), sorghum (*Sorghum bicolor*), and sugarcane (*Saccharum officinarum*) (reviewed in: Rahman et al., 2016; Xu and Shanklin, 2016; Vanhercke et al., 2019). Our previous work generated a high oil (HO) tobacco line that accumulated more than 15% dry weight TAG in leaf tissue by overexpressing: the Arabidopsis transcription factor *WRINKLED1* (*AtWRI1*) that upregulates glycolysis and fatty acid synthesis (Focks and Benning, 1998; Cernac and Benning, 2004; Ma et al., 2013); the Arabidopsis TAG biosynthetic enzyme ACYL-CoA: DIACYLGLYCEROL ACYLTRANSFERASE 1 (*AtDGAT1*) (Katavic et al., 1995; Zou et al., 1999); and the *Sesamum indicum OLEOSIN* gene in a combined push and pull strategy (Vanhercke et al., 2014). The genetic changes in the HO line produced a large accumulation of fatty

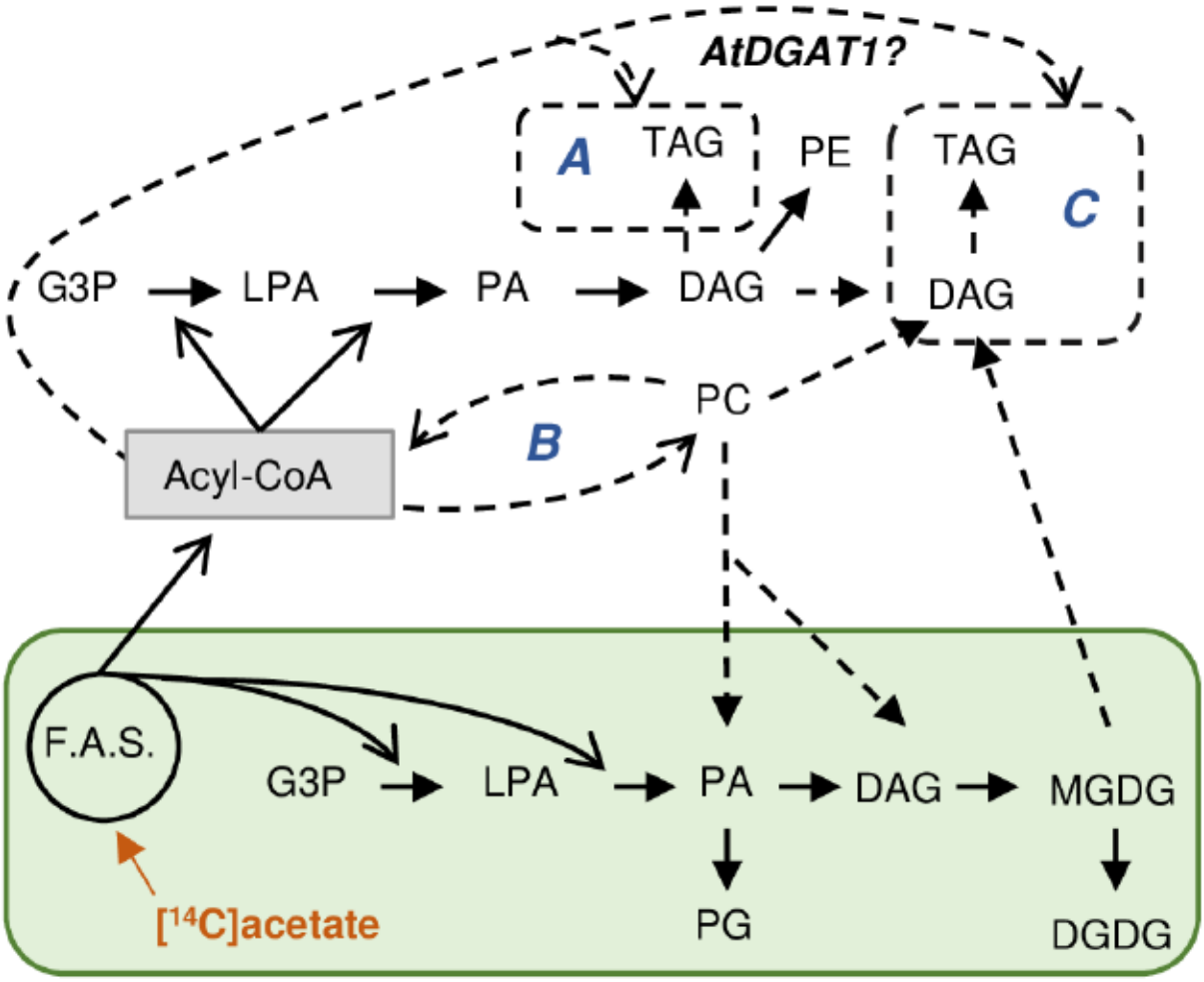

93 acids in leaf TAG. However, the relationship between TAG synthesis and the underlying
94 leaf lipid metabolic network (Fig. 1), including effects on the accumulation of essential
95 leaf photosynthetic membranes, is unknown. The path (or flux) of fatty acids from
96 synthesis in the chloroplast to assembly into TAG in the endoplasmic reticulum (ER) is
97 critical to effectively control the amount and fatty acid composition of TAG without
98 detrimentally affecting membrane production. In particular for plant oil-based biofuels,
99 TAG containing high levels of monounsaturated fatty acids (e.g. oleate, 18:1 (# carbons:
100 # double bonds)) are desirable for the optimal mix of energy density, cold flow
101 properties, and oxidative stability of the fuels (Durrett et al., 2008). The HO leaves
102 accumulate TAG containing ~30% oleate and ~33% polyunsaturated fatty acids (PUFA)
103 (Vanhercke et al., 2014), indicating that substantial improvement of TAG composition

may be possible through further engineering. Changes to the PUFA level in plant TAG are dependent on acyl flux through membrane lipid bound fatty acid desaturases (Bates, 2016), however the impact of enhanced leaf oil production on acyl flux through this biosynthetic network is less clear (Fig. 1).

Plant leaves have two parallel metabolic pathways of glycerol-3-phosphate (G3P) acylation to produce membrane glycerolipids which have been characterized biochemically and genetically over the past 50 years, and reviewed extensively, for example: Roughan and Slack, 1982; Ohlrogge and Browse, 1995; Li-Beisson et al., 2013; Hurlock et al., 2014; Allen et al., 2015; LaBrant et al., 2018; Holzl and Dormann, 2019. In brief, plants synthesize fatty acids while esterified to acyl carrier proteins (ACP) in the plastid. The plastid localized "prokaryotic" pathway of glycerolipid synthesis utilizes acyl-ACPs to esterify 18:1 and 16:0 fatty acids to the *sn*-1 and *sn*-2 positions of G3P respectively, producing first lysophosphatidic acid (LPA), then phosphatidic acid (PA). Phosphatidylglycerol (PG) is produced from prokaryotic PA in the plastid, where only "16:3" plants (including tobacco), also dephosphorylate PA to diacylglycerol (DAG) producing a prokaryotic glycerolipid backbone containing a *sn*-2 16-carbon fatty acid for synthesis of some of the plastid localized galactolipids, monogalactosyldiacyglycerol (MGDG) and digalactosyldiacylglycerol (DGDG) (Mongrand et al., 1998). Plastid localized desaturases produce the 16:3 by desaturation of the 16:0 incorporated into the *sn*-2 position of MGDG and DGDG (Li-Beisson et al., 2013). The glycerolipid backbone for the remaining galactolipids (or all galactolipids in 18:3 plants) is produced by the "eukaryotic" pathway in the endoplasmic reticulum (ER) utilizing ER localized lipid assembly enzymes. In the eukaryotic pathway, free fatty acids are exported from the plastid and activated to acyl-CoAs prior to utilization by extra-plastidic acyltransferases. The production of PA parallels that of the prokaryotic pathway except that 18-carbon fatty acids are found at both *sn*-1 and *sn*-2. Any 16:0 present is localized to the *sn*-1 position (Frentzen et al., 1983), and is not further desaturated. Subsequent dephosphorylation of PA produces the eukaryotic DAG backbone for synthesis of the major ER membrane lipids phosphatidylcholine (PC) and phosphatidylethanolamine (PE) (Li-Beisson et al., 2013). The production of eukaryotic galactolipids involves the plastid localized assembly of MGDG from a eukaryotic DAG moiety derived from PC,

although the exact lipid that is transported from the ER to the plastid is unclear, but could be PC, or the PC-derived intermediates PA or DAG (Hurlock et al., 2014; Maréchal and Bastien, 2014; LaBrant et al., 2018; Karki et al., 2019).

Direct production of leaf TAG containing oleate in the HO tobacco line could occur through utilization of newly synthesized oleoyl-CoA by the Kennedy pathway (Fig. 1A); however, the presence of PUFA in HO TAG indicates that other mechanisms of acyl flux must be involved. Reactions which exchange acyl groups on and off PC are integral to the eukaryotic pathway. PC is the site of ER localized fatty acid desaturation of oleate ($18{:}1^{\Delta 9}$) to make the PUFAs linoleate ($18{:}2^{\Delta 9,12}$) and α-linolenate ($18{:}3^{\Delta 9,12,15}$) (Li-Beisson et al., 2013). PUFAs can enter the acyl-CoA pool to be used by the eukaryotic pathway acyltransferases through a PC deacylation and lyso-PC acylation cycle coined "acyl editing" (Fig. 1B) (Bates et al., 2007). Through acyl editing oleate is incorporated into PC for desaturation, and the corresponding PUFA can reenter the acyl-CoA pool to be used for the synthesis of glycerolipids by Kennedy pathway reactions (Bates, 2016). Quantitative analysis of acyl flux through the eukaryotic pathway with *in vivo* metabolic labeling has indicated that most nascent fatty acids first are incorporated into PC through acyl editing prior to acylation of G3P, and that fatty acid flux around the acyl editing cycle is the largest lipid metabolic flux in many plant tissues including: developing pea (*Pisum sativum*) leaves (Bates et al., 2007); soybean (*Glycine max*) and camelina (*Camelina sativa*) embryos (Bates et al., 2009; Yang et al., 2017); and Arabidopsis seeds, leaves, and cell cultures (Bates et al., 2012; Tjellström et al., 2012; Wang et al., 2012; Karki et al., 2019). Mechanisms of acyl transfer from membrane lipids into TAG also include membrane lipid turnover resulting in DAG containing PUFAs that are used for TAG biosynthesis (Fig. 1C) (Bates, 2016). In various oilseed tissues PC-derived DAG is the major source for TAG synthesis (Bates et al., 2009; Bates and Browse, 2011; Yang et al., 2017). In leaves, DAG derived from chloroplast galactolipids can also be used to produce TAG by homeostatic mechanisms (Xu and Shanklin, 2016), and during stress (Sakaki et al., 1990; Moellering et al., 2010; Narayanan et al., 2016; Arisz et al., 2018). Thus, the composition of TAG produced in leaves is a consequence of the relative rates of acyl flux through various membrane lipid pools, and the relative rate of fatty acid desaturation within these lipid pools.

The expression of the genes encoding AtWRI1, AtDGAT1, and sesame OLEOSIN have led to an increased level of fatty acid synthesis and accumulation of TAG in leaves of the HO tobacco line (Vanhercke et al., 2014). Transcriptomic analysis of the HO line indicated upregulation of glycolysis and fatty acid synthesis (Vanhercke et al., 2017), consistent with the function of WRI1 in plant tissues (Focks and Benning, 1998; Ma et al., 2013). However, there was little to no change in expression of the acyltransferases involved in TAG and membrane lipid assembly (Vanhercke et al., 2017). Previous studies have indicated that transcript abundance may not correlate with protein levels (Hajduch et al., 2010; Vogel and Marcotte, 2012), and transcript abundance alone is a poor indicator of metabolic flux (Fernie and Stitt, 2012; Schwender et al., 2014; Allen et al., 2015). Thus, the path of acyl flux through the lipid metabolic network into TAG is unclear (Fig. 1A-C), including if turnover of the abundant chloroplast lipids in leaves may be feeding TAG biosynthesis. Future leaf oil engineering efforts may need to specifically target these facets of the lipid metabolic network to optimize leaf TAG accumulation and composition. Therefore, to better understand the pathways of acyl flux in wild-type tobacco leaves, and how these pathways are altered when accumulating high levels of leaf TAG in the transgenic HO line, we performed a series of *in vitro* enzymatic assays, and *in vivo* continuous pulse and pulse-chase metabolic labeling studies that provide new insights into tobacco leaf lipid metabolism and its engineering.

Results

Engineering leaf TAG accumulation also effects the accumulation of leaf membrane lipids

The HO line has a large increase in leaf TAG accumulation (Vanhercke et al., 2014), which was confirmed in the current effort. Our results indicate that the boost in TAG was accompanied by changes to leaf membrane lipid abundance (Fig. 2). PC and DAG increased whereas other membrane lipids including the galactolipids that are the bulk of the chloroplast photosynthetic membranes, decreased, compared to the wild-type (WT) (Fig. 2A). The difference in lipid abundance was also reflected through changes in fatty acid compositions (Fig. 3). Total leaf fatty acid composition (Fig. 3A) of the HO line reflected alterations in the fatty acid composition of TAG (Fig. 3B) which accumulated as the major lipid product (Fig. 2A). PC had a notable decrease in the unsaturation index as 18:3 decreased and 18:1 significantly increased (Fig. 3C). MGDG 16:3 content decreased by half and 18:2 significantly increased (Fig. 3D). The change in MGDG fatty acid composition was predominantly due to a reduction in 16-carbon fatty acids at the *sn*-2 position, indicating an ~40% reduction in the proportion of prokaryotic pathway produced MGDG (Supplemental Fig. S1A-C).

Considering that acyl and glycerol flux through PC is key to producing other membrane lipids, we calculated the ratio of membrane lipids to PC (Fig. 2B). The lipid/PC ratios dropped in the HO line and indicated a change in the redistribution of fatty acid from PC to other lipids, though it is less clear if this is a consequence of reduced biosynthesis, or enhanced turnover, or both. To better understand the changes in the lipid metabolic network that accommodate TAG accumulation, the flux of acyl groups through the lipid metabolic network was analyzed by both *in vitro* assays and *in vivo* tracing of leaf lipid metabolism in the WT and HO line.

A direct linear Kennedy pathway of TAG biosynthesis is not active in WT or HO leaf microsomes

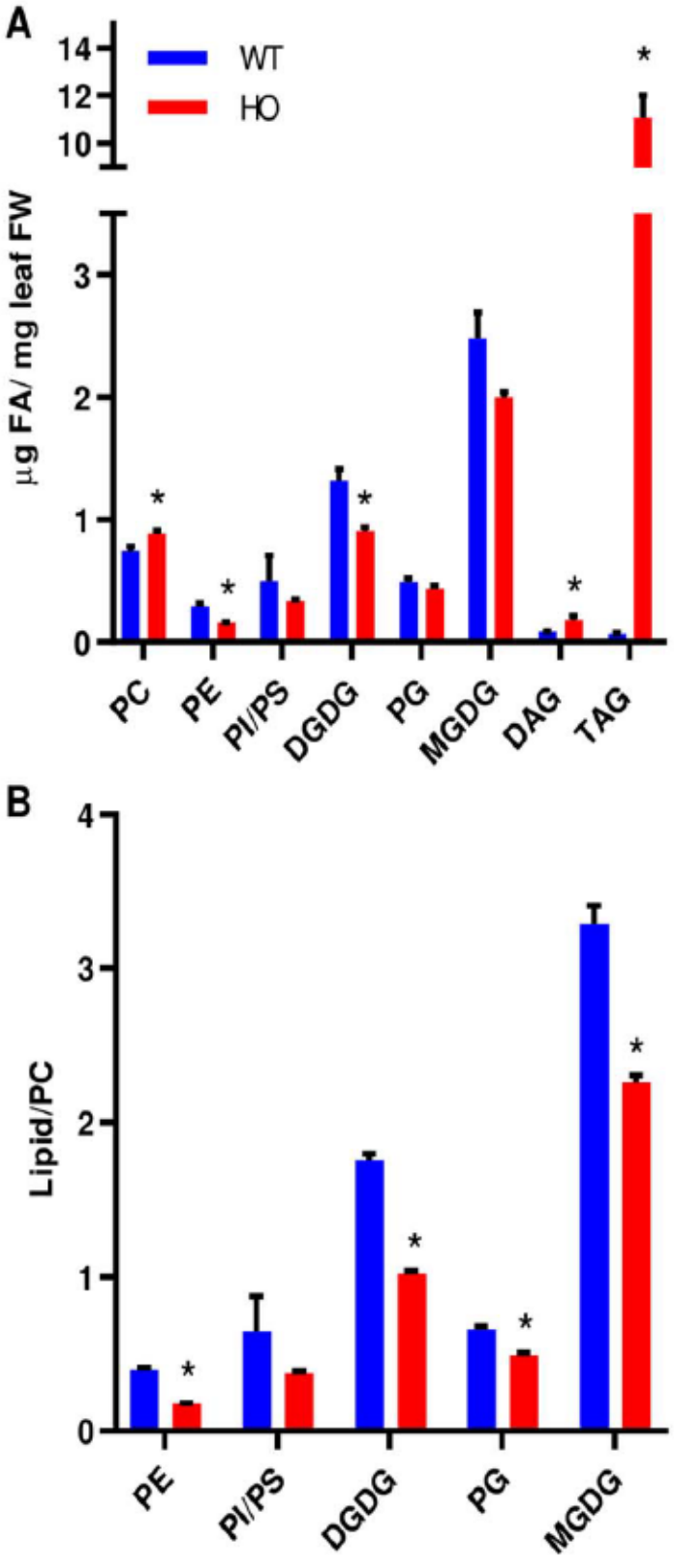

219 Microsomal studies have been invaluable in characterizing enzymatic functions

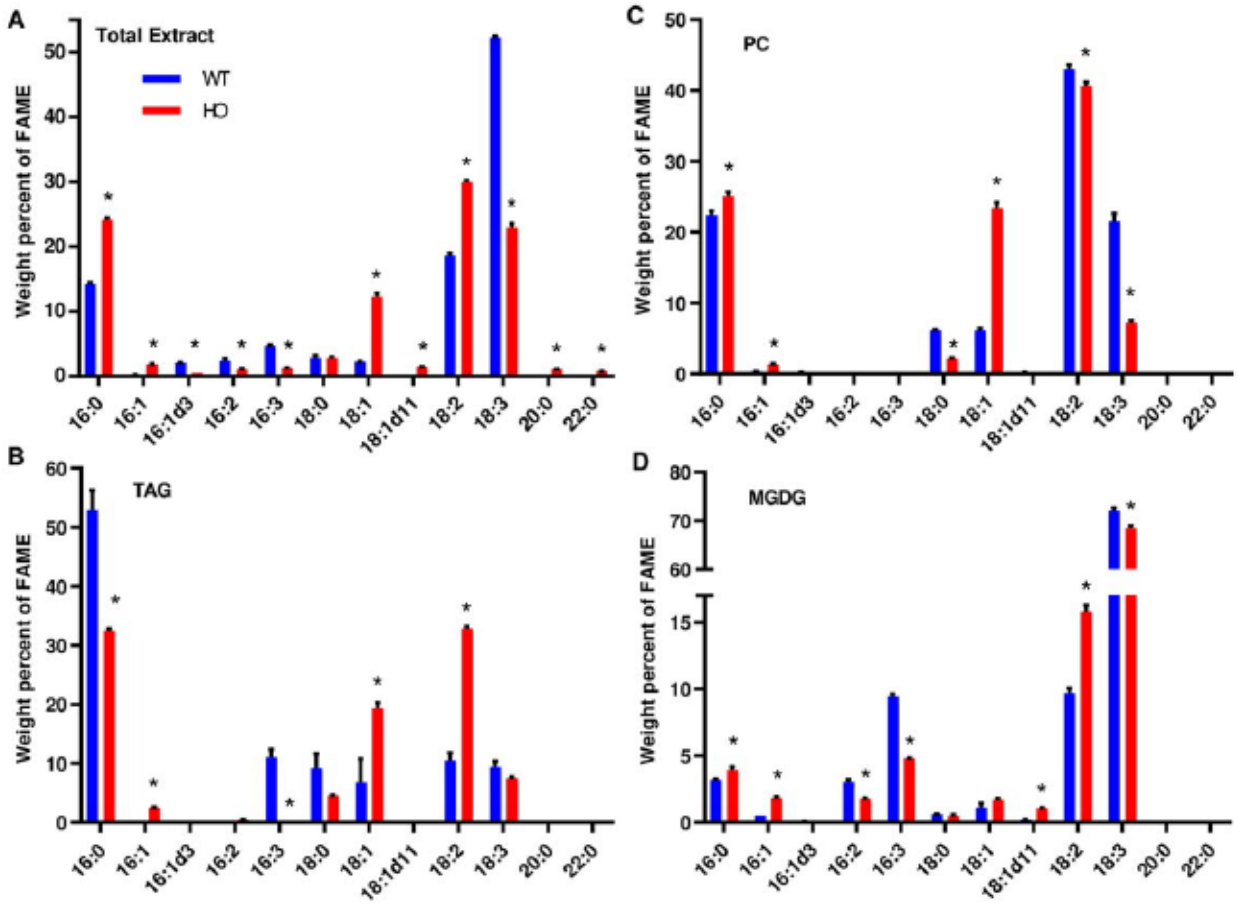

that produce TAG through the linear Kennedy pathway in plants (Barron and Stumpf, 1962; Stymne and Stobart, 1984; Bafor et al., 1991). To determine if a direct Kennedy pathway of TAG biosynthesis (Fig. 1A) is present, we assayed WT and HO tobacco leaf microsomes for TAG production with [^{14}C]G3P and 18:1-CoA (Fig. 4). No significant TAG accumulation was detected within a 60 min assay, though the total label in lipids produced by HO microsomes was approximately 5-fold higher than that in the WT suggesting an overall upregulation in *de novo* glycerolipid assembly. In the HO line PA was the major labeled product, suggesting that PA conversion to DAG may be limiting in the isolated microsomes. The *in vitro* results indicate that efficient channeling of substrates into TAG through a Kennedy pathway (Fig. 1A) may not occur in the HO line; however, since some proteins can be lost during microsomal preparation, additional *in vivo* pulse and pulse-chase metabolic labeling experiments were performed to further study the acyl flux through lipids.

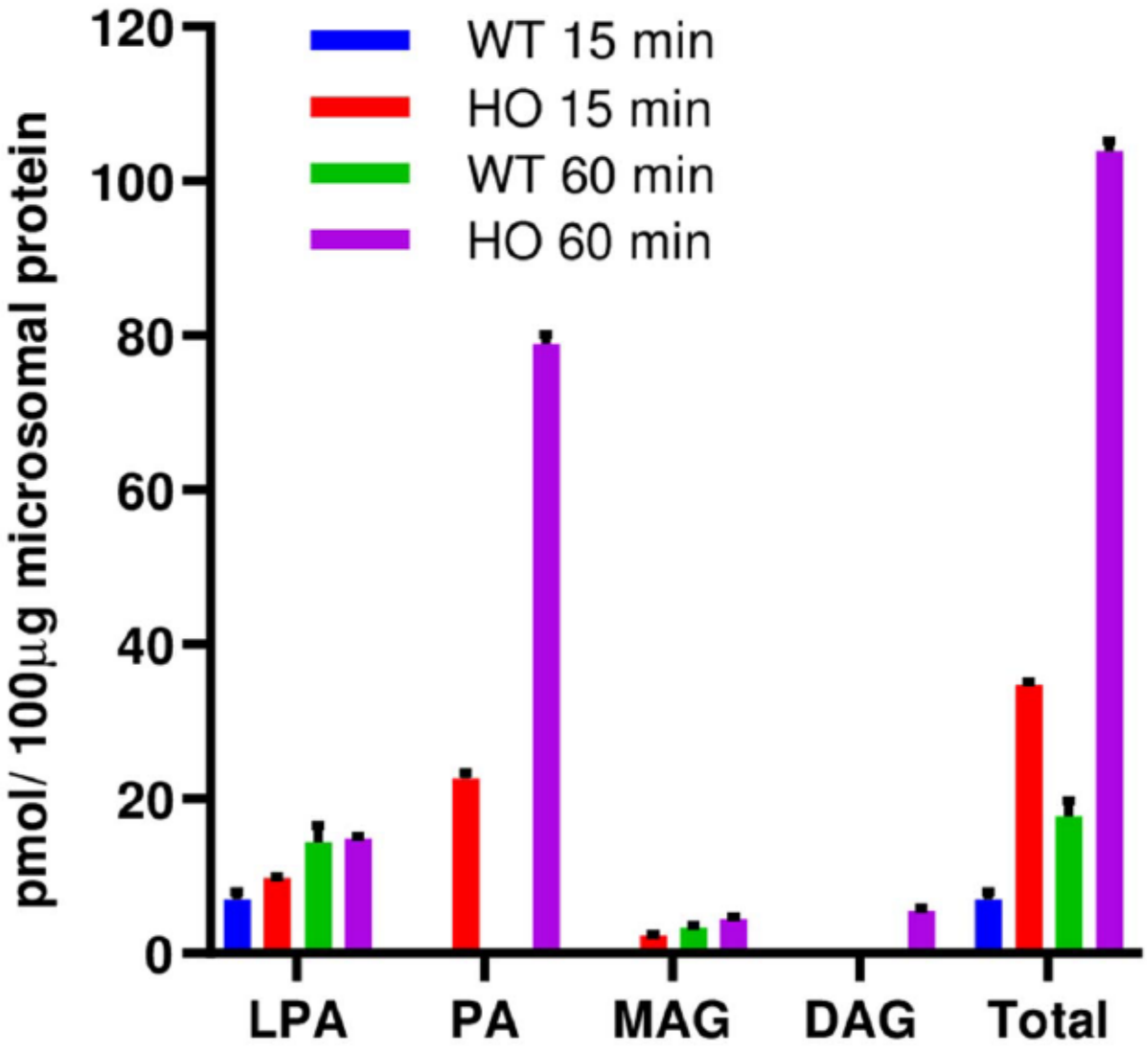

TAG accumulation alters the relative flux of nascent fatty acids into the eukaryotic and prokaryotic pathways of glycerolipid assembly

To understand how the push and pull engineering approach to produce leaf TAG (Vanhercke et al., 2014) affects the initial flux of newly synthesized fatty acids into the endogenous leaf lipid metabolic network (Fig. 1), we performed a continuous [^{14}C]acetate metabolic labeling of 3-120 minutes on leaf disks from 66-day-old WT and HO plants. [^{14}C]acetate is incorporated into the acetyl-CoA pool utilized for fatty acid

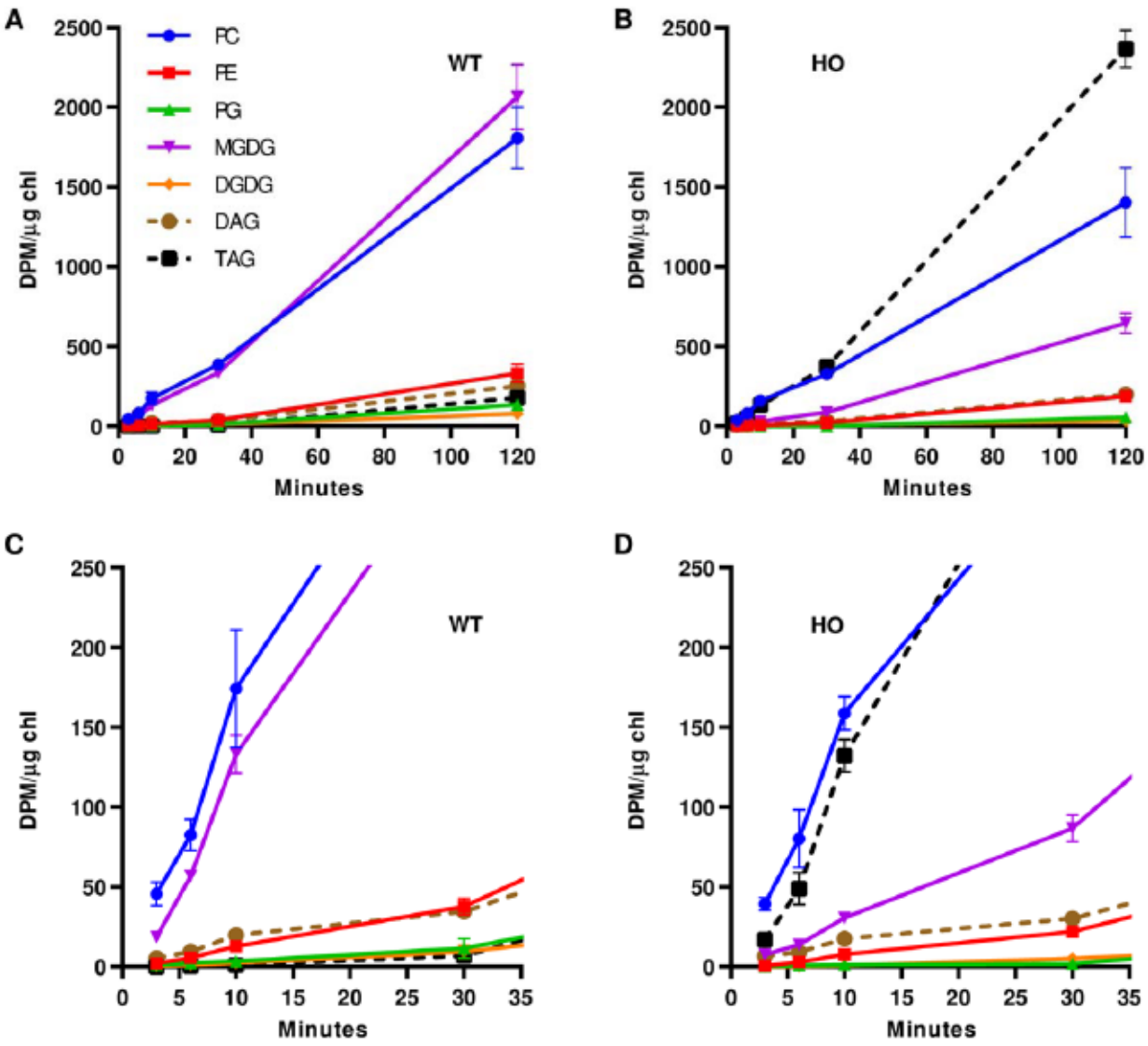

synthesis (Fig. 1), and short time point labeling is instructive for characterizing the initial steps of nascent acyl flux into the lipid metabolic network (Allen et al., 2015). Total incorporation of [^{14}C]acetate into leaf lipids was linear for both the WT and the HO line over the 120 min time course, and there was no statistical difference in total label between genotypes at any time point (Supplemental Fig. S2). However, linear regression indicated slopes of 50.5 ± 1.9 DPM µg chlorophyll^{-1} min^{-1} in the WT, and 43.1 ± 1.3 DPM µg chlorophyll^{-1} min^{-1} in the HO line. The slopes were significantly different with a p-value = 0.0035. The reason for the reduced slope of [^{14}C]acetate incorporation into lipids of the HO line is not immediately clear, however it could be due to dilution of the exogenous [^{14}C]acetate by the much larger flux of endogenous carbon into acetyl-

CoA and fatty acid production in the HO leaf cells compared to that in the WT. Therefore, we normalized the total accumulation of HO lipids to the WT average total lipid accumulation at each time point (Fig. 5) so that the relative rates of synthesis of individual lipid classes between the genotypes could be compared. The normalization slightly increased the total DPM μg chlorophyll^{-1} in each lipid class, but the pattern of lipid synthesis essential for determining precursor-product relationships was unchanged regardless of whether data was normalized (Fig. 5) or not (Supplemental Fig. S3).

In WT leaves most newly synthesized fatty acids accumulate in PC and MGDG across the time course with only minor amounts in TAG (Fig. 5A). At early time points PC is the major labeled lipid (Fig. 5C), and both PC and MGDG accumulate labeled fatty acids at similar initial rates (Table 1) but by 120 min MGDG accumulates more label (Fig. 5A, 5C). These results are consistent with: 1) PC as a first product of nascent fatty acid incorporation into ER lipids (Bates et al., 2007; Tjellström et al., 2012); 2) *de novo* synthesis of MGDG through the prokaryotic pathway; and 3) the precursor-product relationship of PC and MGDG over time as acyl groups move through the eukaryotic pathway of galactolipid synthesis (Li-Beisson et al., 2013). All other membrane lipids initially accumulated little radiolabel, but slowly increased over time. This is consistent with the redistribution of nascent fatty acids from PC to other lipids through acyl editing (Bates et al., 2007; Bates, 2016), and the conversion of MGDG to DGDG within the plastid (Kelly and Dormann, 2004; Hurlock et al., 2014; LaBrant et al., 2018).

The incorporation of nascent fatty acids into lipids of HO leaves was dramatically different (Fig. 5B, 5D). Similar to the WT, in the HO line PC was the most labeled lipid at the earliest time points (Fig. 5D) and had a similar rate of label accumulation (Table 1). However, the next most labeled lipid was TAG (rather than MGDG of the WT, Fig. 5C) and the initial rate of nascent fatty acid incorporation into TAG was 119-fold higher than in the WT (Table 1). At the 3 min time point there was over twice the amount of nascent fatty acids in PC (39.5 ± 3.9 DPM/μg chl) than TAG (17.0 ± 4.4 DPM/μg chl). However, the accumulation of labeled fatty acids in TAG continued to accelerate surpassing PC by 15 min, and by 120 min TAG accumulated 1.7-fold more labeled fatty acids than PC, representing ~48% of total labeled lipids (Fig. 5B, 5D). This result is consistent with the very large mass accumulation of TAG in HO leaves (Fig. 2). Despite the larger mass

accumulation of TAG over time, the more rapid labeling of PC at initial time points suggests a PC-TAG precursor-product relationship for fatty acid flux.

PE which is produced in the ER through the eukaryotic pathway similar to PC and TAG, did not have a significant difference in the rate of synthesis with nascent fatty acids in the WT and the HO line (Table 1). However, there was a significant decrease in the rates of nascent fatty acid incorporation into chloroplast lipids MGDG (-4.9 fold), DGDG (-2.5 fold), and PG (-1.9 fold) (Fig. 5, Table 1) in the HO line as compared to the WT. For each of these lipids the initial rates of labeling represents synthesis through the prokaryotic pathway, whereas eukaryotic pathway synthesis occurs over much longer time scales as labeled fatty acids move through PC and ER-derived lipids and eventually return to the chloroplast (Browse et al., 1986). Therefore, the results suggest a shift in fatty acid allocation to the eukaryotic pathway over the prokaryotic pathway for the production of TAG in the transgenic line.

In Figure 6 we estimated the relative flux of nascent fatty acids into the eukaryotic and prokaryotic glycerolipid assembly pathways by comparing the accumulation of label in ER localized (PC, PE, TAG) and plastid localized (MGDG, DGDG, PG) lipids. The metabolic labeling of WT leaves showed that nascent fatty acids accumulated into ER lipids at a slightly greater rate than plastid lipids (Fig. 6A). Linear regression of the initial phase of glycerolipid assembly (first 10 min) indicated that flux of newly synthesized fatty acids into glycerolipids was 20.3 ± 4.6 and 17.1 ± 1.5 DPM μg chlorophyll^{-1} min^{-1} for ER and plastid lipids, respectively. The initial ER/plastid ratio at 3 min of labeling was ~2.4 but dropped to 1.3 by 10 min. This change is likely reflected by the lipids quantified at these time points. In the eukaryotic pathway nascent fatty acids exported from the plastid are initially directly incorporated into PC, but in the prokaryotic pathway nascent fatty acids are first incorporated into LPA, PA, and DAG prior to MGDG synthesis (Allen et al., 2015). Considering that lipid classes LPA, PA, and DAG occur in both pathways (Fig. 1) they were not included in the analysis. Therefore, the lag in acyl flux through intermediates of the prokaryotic pathway at short time points may explain the ratio favoring the eukaryotic pathway at short time points. The changing ratio of labeled fatty acids in ER/plastid lipids stabilized by 10 min, then slowly decreased over the time course. However, in the HO line the relative initial rate of newly

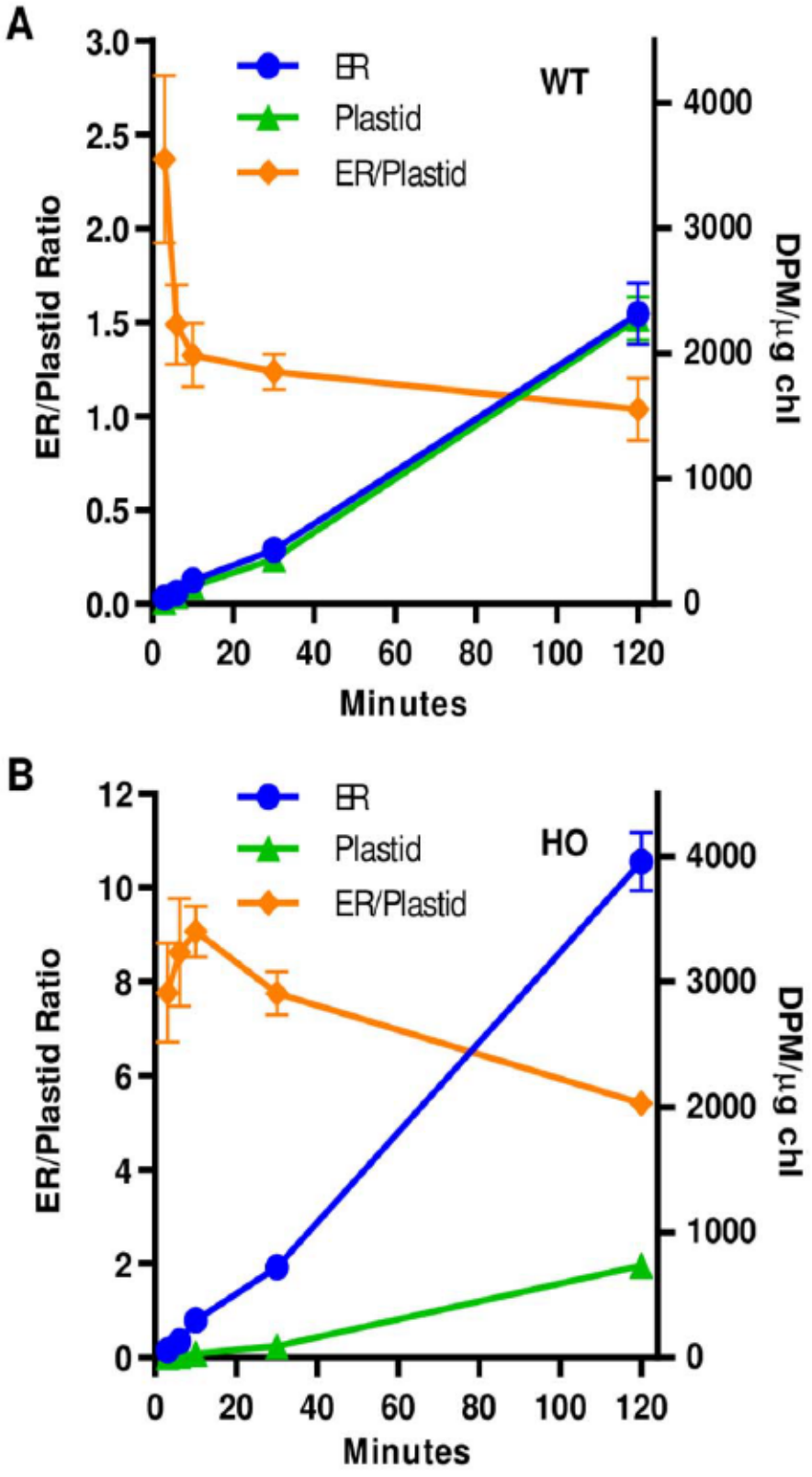

314 synthesized fatty acid accumulation in ER and plastid lipids was 34.9 ± 4.6 and 3.6 ± 15

315 0.6 DPM µg chlorophyll^{-1} min^{-1}, respectively. Thus, the eukaryotic pathway accounted
316 for a 9-fold higher flux of fatty acids into glycerolipids than the prokaryotic pathway of
317 the HO line. Similar to the WT, in the HO line the ER/plastid ratio for labeled fatty acid
318 accumulation stabilized by 10 min and then decreased over the time course (Fig. 6B).
319 The decrease in the ER/plastid ratio over time in both genotypes likely represents the
320 PC-galactolipid precursor-product relationship of the eukaryotic pathway.

321 In Figure 5 and 6, the accumulation of newly synthesized fatty acids in MGDG
322 can be due to both the prokaryotic and eukaryotic pathways. To determine if the
323 reduction in accumulation of labeled MGDG is due to reduced acyl flux through the
324 prokaryotic, eukaryotic, or both pathways we collected MGDG from the 30 and 120 min
325 time points and analyzed the radioactivity in individual molecular species (Supplemental
326 Fig. S4 and S5). The prokaryotic pathway initially produces the 18:1/16:0 molecular
327 species of MGDG which is further desaturated to predominantly 18:3/16:3 (Ohlrogge
328 and Browse, 1995). Eukaryotic MGDG is indicated to be synthesized from a
329 polyunsaturated-containing-DAG ultimately derived from PC, and is further desaturated
330 to predominantly 18:3/18:3 in the plastid (Slack et al., 1977; Ohlrogge and Browse,
331 1995). Therefore, 18/16-carbon-containing molecular species are representative of the
332 prokaryotic pathway, and 18/18-carbon molecular species are representative of the
333 eukaryotic pathway. The accumulation of MGDG through each pathway is summarized
334 in Table 2. The analysis of MGDG molecular species gave four insights into the acyl flux
335 through the prokaryotic and eukaryotic pathways: (1) the HO line had a reduced
336 proportion of prokaryotic MGDG molecular species (and thus increased eukaryotic
337 proportion) as compared to the WT; (2) however with the very large decrease in total
338 ^{14}C-MGDG accumulation (Fig. 5), the total acyl flux into MGDG through the eukaryotic
339 pathway was reduced by over 30% and acyl flux through the prokaryotic pathway was
340 reduced by over 70% (Table 2); (3) both lines had an increase in eukaryotic molecular
341 species from 30 to 120 min of labeling (Table 2) consistent with the role of the
342 eukaryotic pathway for PC turnover to produce plastid galactolipids, and consistent with
343 the decrease in the ER/plastid accumulation ratio of Fig. 6; (4) the profile of prokaryotic
344 and eukaryotic MGDG molecular species in the HO line suggested a reduced rate of
345 plastid desaturation, as compared to the WT (Supplemental Fig. S5). Therefore, an

346 increase in the total flux of newly synthesized acyl groups into ER lipids (mostly TAG,
347 Fig. 5, 6), and a reduction in acyl flux into plastid lipids through both the prokaryotic and
348 eukaryotic pathways (Table 2) contributed to the dramatic redistribution of acyl flux
349 through the lipid metabolic network in the HO tobacco line.
350
351 **Regiochemical analysis indicates limited changes in pathway structure for initial**
352 **steps of ER glycerolipid assembly**
353
354 To better understand which branches of the lipid metabolic network (Fig. 1) are
355 involved in the altered flux of nascent fatty acids into membrane lipids and TAG of the
356 HO line as compared to the WT, we performed regiochemical analysis (Fig. 7) of
357 labeled DAG, PC and TAG across the [^{14}C]acetate labeling time course from Fig. 5. In
358 both the WT and the HO line newly synthesized fatty acids were initially incorporated
359 more on the *sn*-1 position relative to the *sn*-2 position of the total labeled DAG pool, but
360 this was quickly equilibrated to approximately equal distribution by 10 min (Fig. 7A, B),
361 and there was no statistical difference in stereochemical labeling in DAG between the
362 lines. The higher initial labeling of DAG *sn*-1 position over *sn*-2 has previously been
363 reported in the predominantly eukaryotic *de novo* DAG pools of developing soybean
364 embryos and Arabidopsis seeds (Bates et al., 2009; Bates et al., 2012). Rapid
365 equilibrium of labeling across stereochemical positions in tobacco plants may also
366 represent a substantial contribution of prokaryotic DAG which is produced from only
367 nascent fatty acids (Ohlrogge and Browse, 1995), and thus the labeled fatty acids will
368 be evenly distributed across both positions as demonstrated for prokaryotic lipids in
369 rapeseed (*Brassica napus*) leaves (Williams et al., 2000). In contrast to DAG, newly
370 synthesized fatty acids accumulated predominantly in the *sn*-2 position of PC across the
371 time course in both plants (~63-70% WT and 67-76% HO). The slightly more nascent
372 fatty acids at the *sn*-2 position of PC in the HO line was only significant at the 3- and
373 120-min time points (Fig. 7C, D). The PC stereochemical labeling is consistent with
374 previous leaf, seed, and cell culture analyses where a single nascent fatty acid is initially
375 incorporated next to a previously synthesized fatty acid within PC (with preference for
376 *sn*-2 over *sn*-1) through acyl editing as nascent fatty acids leave the plastid (Bates et al.,

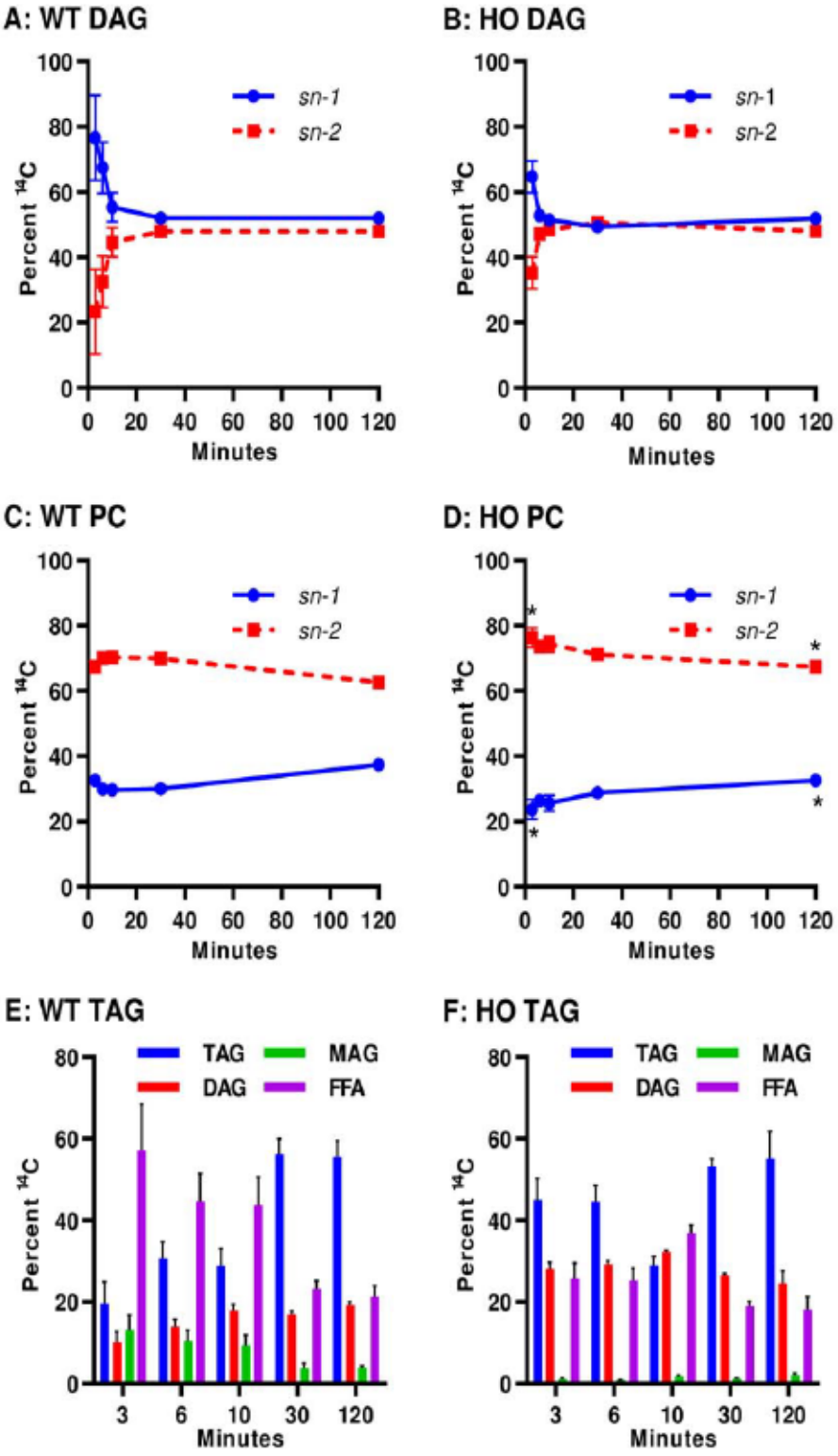

377 2007; Bates et al., 2009; Bates et al., 2012; Tjellström et al., 2012; Allen, 2016; Bates,

2016; Karki et al., 2019).

Partial TAG lipase digestions of labeled TAG from both plants revealed that most labeled acyl groups were released by the lipase in the free fatty acid fraction (*sn*-1 or *sn*-3) and little remained in the monoacylglycerol fraction (*sn*-2) (Figure 7E, F). Considering the similar labeling of the *sn*-1 and *sn*-2 position of DAG, the low *sn*-2 labeling of TAG suggests that most TAG labeling within this short time course represents incorporation of a newly synthesized radiolabeled fatty acid onto the *sn*-3 position of an unlabeled DAG molecule, and does not reflect the rapidly produced eukaryotic *de novo* DAG that might be expected from a direct Kennedy pathway of TAG synthesis (Fig. 1A). Together the DAG, PC and TAG regiochemical analysis suggests that even though there are big differences between the WT and the HO line for the quantity of acyl flux into eukaryotic pathway lipids, the initial steps of eukaryotic glycerolipid assembly (or the initial structure of the eukaryotic lipid network) between these genotypes do not vary considerably.

Nascent acyl groups initially incorporated into PC are redistributed differently between the WT and the HO line.

The short time point [^{14}C]acetate labeling in Fig. 5 demonstrated that a majority of newly synthesized fatty acids are initially incorporated into PC of both genotypes. The redistribution of fatty acids from PC to other lipids over time was assessed through an additional pulse-chase experiment (Fig. 8, Fig. 9). Leaf disks of 73-day-old plants were pulsed with [^{14}C]acetate for 0.5 hours, rinsed and incubated without the radiolabel for up to 22 hrs. In both plants the total ^{14}C-labeled lipids increased throughout the pulse and chase periods (Fig. 8). During the pulse, labeled lipids accumulated at the most rapid rates (4800 ± 500 and 9600 ± 900, DPM μg chlorophyll^{-1} hr^{-1} in WT and HO, respectively). During the first 2 hrs of the chase period the rate of labeled lipid accumulation was reduced 6-7 fold to 840 ± 210 and 1300 ± 340 DPM μg chl^{-1} hr^{-1} in WT and HO leaves respectively, which likely represents continued uptake of [^{14}C]acetate during the washes. Finally from 2-22 hrs radiolabel accumulated at even slower but constant rates of 330 ± 90 and 250 ± 50 DPM μg chl^{-1} hr^{-1}, which may

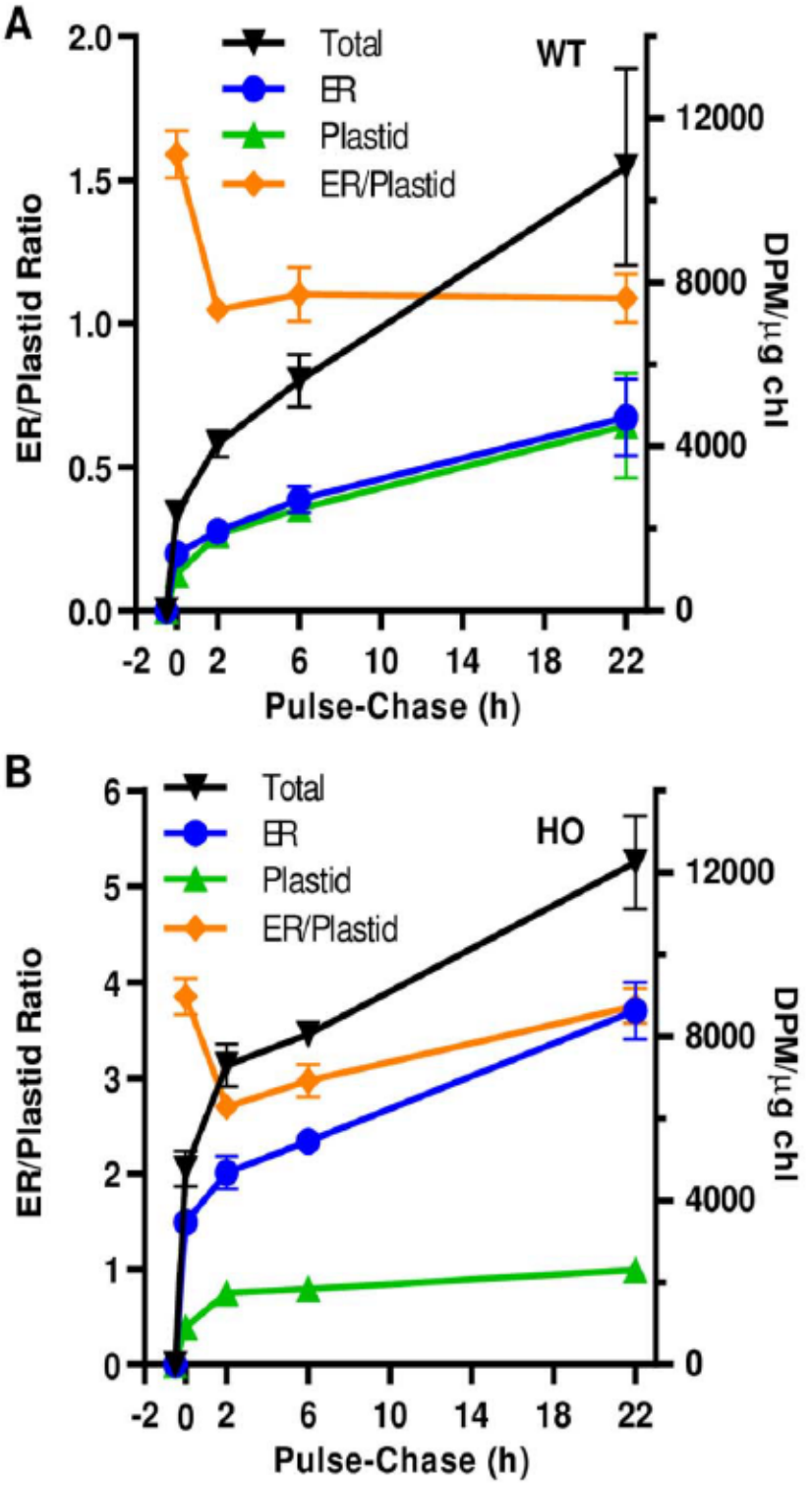

409 represent continued utilization of a pool of [^{14}C]acetate that was taken up into the leaf

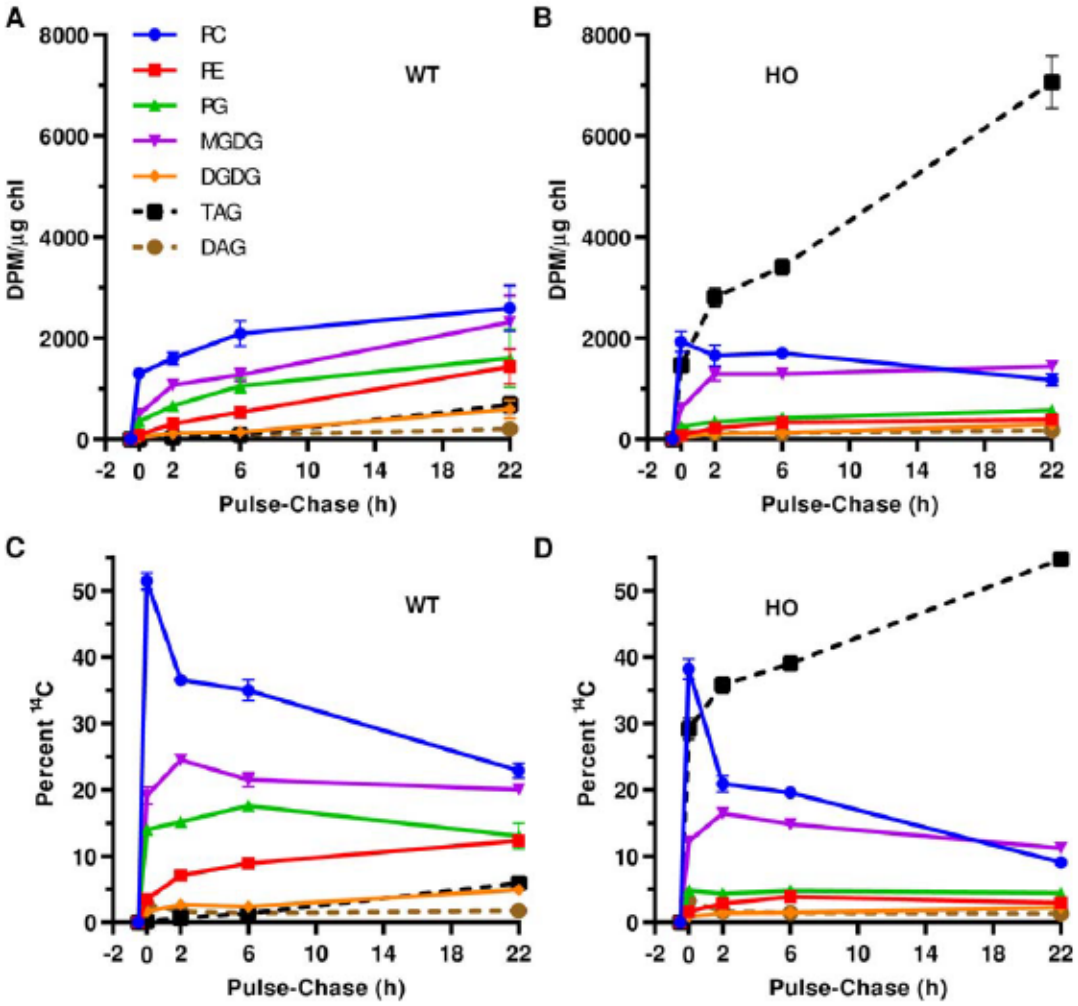

410 tissue during the pulse but utilized at a slower rate, as compared to the bulk of the
411 [^{14}C]acetate substrate. Therefore, the experiment should be considered a rapid ^{14}C
412 pulse that is followed by labeling with a significantly lower concentration of [^{14}C]acetate
413 (15-38 fold lower based on initial and final rates). This distinction is relevant when
414 comparing the total accumulation of radiolabel in individual lipid classes (Fig. 9A-B) to
415 the relative radiolabel accumulation between lipid classes in each genotype (Fig. 9C-D).
416 Similar to the short time point pulse experiment (Fig. 5, Fig. 6), the HO line accumulated
417 labeled fatty acids predominantly in ER lipids across the time course, whereas labeling
418 of ER and plastid lipids was similar across the time course in the WT (Fig. 8).

In the WT all individual lipid classes accumulated ^{14}C acyl groups during the pulse-chase but at different rates across the time course (Fig. 9A). At the end of the pulse, PC contained the most ^{14}C with over 2.6-fold more ^{14}C than any other lipid, but the rate of labeled fatty acid accumulation in PC continued to slow down across the chase time course. During the chase, the accumulation of ^{14}C fatty acids increased in MGDG relative to PC such that by the end of the time course they contained similar amounts of total labeled fatty acids. The results are consistent with the PC-MGDG precursor-product relationship of the eukaryotic pathway in leaves, and the redistribution of nascent acyl groups from PC to other ER localized lipids through acyl editing (Fig. 1). In HO leaves the [^{14}C]acetate pulse-chase results are distinct. Initially PC contained the most label after the pulse but was surpassed by TAG before the 2 hr time point (Figure 9B, D). By the end of the 22 hr chase period TAG accumulated ≥ 4.9-fold more ^{14}C fatty acids than any other lipid. Even though the total lipid labeling is increasing over the chase period (Fig. 8B), the amount of labeled fatty acids in PC of the HO line decreases over the whole chase period (Figure 9B). The difference in accumulation of ^{14}C fatty acids in PC between the WT and the HO line suggests that PC turnover and redistribution of acyl groups occurs at a higher rate in the HO line. All other membrane lipids in HO leaves increased slightly during the chase (Fig. 9B), but much less than in WT leaves. In the WT, PC and MGDG had a clear precursor-product relationship of acyl flux that is not directly evident in the HO line of Fig. 9B. To determine if the small increases in HO MGDG ^{14}C acyl accumulation are due to (1) the continued synthesis of ^{14}C fatty acids and their incorporation into the metabolic network during the chase (Figure 8B); or (2) are due to a reduced redistribution of acyl label from PC, we compared the labeled MGDG molecular species distribution at the 0 and 22 hr time points (Supplemental Figure S6, summarized in Table 3). After the 30 min pulse, the proportion of eukaryotic and prokaryotic MGDG molecular species in both the WT and the HO line was similar to that of the 30 min continuous labeling time point (Table 2). During the 22 hr chase period in the WT, the eukaryotic MGDG molecular species increased 3-fold as a proportion (Table 3), consistent with the PC-MGDG precursor-product relationship of the eukaryotic pathway. However, during the chase in the HO line, the proportion of eukaryotic MGDG molecular species only increased 1.5-fold

(Table 3). Therefore, the reduced accumulation of MGDG in the HO line during the chase (Fig. 9B) is also consistent with a reduced redistribution of acyl groups from PC to MGDG through the eukaryotic pathway MGDG.

Pulse-chase experiments are commonly represented as the percent labeling in the different products over time (Figure 9C, D), yet the interpretation is dependent on the relative accumulation of the total lipids (Fig. 8A, B) and each individual lipid (Fig. 9A, B) over the chase period. In both genotypes PC had the largest decrease in proportional labeling, consistent with the conclusions from above that acyl groups are redistributed from PC to other lipids over the time course. However, considering that nascent ^{14}C acyl groups continue to enter the system over the chase (Fig. 8) and are predominantly incorporated into PC first (Fig. 5, Fig. 9), the actual turnover of PC is greater than the apparent turnover of half of the labeled PC in the WT, and over 76% of the labeled PC in HO leaves. In addition, the proportional labeling of MGDG in both genotypes also decreased from 2-22 hrs of the chase. This represents both the MGDG-DGDG precursor-product relationship of lipid synthesis (Li-Beisson et al., 2013), as well as the continual incorporation of labeled acyl groups into predominantly PC of the WT, and both PC and TAG of the HO line. Hence the apparent 32% decrease in MGDG accumulation in the HO line does not indicate that MGDG is turning over to feed the large increase in TAG accumulation, but it is the result of the labeled acyl group accumulation predominantly in TAG as more fatty acids are synthesized over the time course (Fig. 8). Therefore, the combined HO pulse-chase results indicate that TAG synthesis draws acyl groups predominantly from PC turnover (Fig. 9B, 9D), which may compete with eukaryotic pathway MGDG synthesis for acyl groups (Table 3), but there does not appear to be evidence of galactolipid turnover providing substrates for TAG biosynthesis.

Discussion

Biotechnology may help to meet societal needs by engineering metabolism to enhance the production of biological resources for food or industry. Plant lipids can be one part of this solution through increased oil yields per area of land for biofuel production. The current state of vegetative oil engineering involves the expression of only a few genes including: transcription factors to increase fatty acid synthesis, DGAT to convert DAG to TAG, and oleosin to prevent TAG breakdown in a push-pull-protect strategy (Vanhercke et al., 2014; Xu and Shanklin, 2016; Vanhercke et al., 2017). However, TAG biosynthesis requires many additional enzymatic steps that directly overlap with essential membrane lipid production (Fig. 1, (Bates and Browse, 2012)), and quantitative analysis of the oil end product does little to explain the metabolic path fatty acids take to accumulate in TAG. It is also unclear how an introduced DGAT fits into the leaf lipid metabolic network designed to accumulate ER and chloroplast membrane lipids, or which substrate pools are used in TAG biosynthesis (Fig. 1). For biofuel production, newly synthesized 18:1 could be directly incorporated into TAG with a minimal number of enzymatic steps using the Kennedy pathway (Fig. 1A), however this would not account for the presence of 18:2 and 18:3 measured in TAG. To understand the path of acyl flux through the lipid metabolic network in WT tobacco leaves, and how the engineered changes in HO affect acyl flux, we analyzed the mechanisms of acyl flux in WT and HO leaves.

A Kennedy pathway of TAG assembly is not present in HO leaves

TAG composed of oleate is a desirable quality for biofuel production (Durrett et al., 2008). The least number of steps to incorporate oleate into TAG is directly through the Kennedy pathway reactions: glycerol-3-phosphate acyltransferase (GPAT) and lysophosphatidic acid acyltransferase (LPAT) to produce PA, dephosphorylation by phosphatidic acid phosphatase (PAP) to produce DAG, and acylation of DAG by to produce TAG. (Fig. 1A (Bates, 2016)). The large increase in 16:0 and 18:1 in HO TAG suggests that a Kennedy pathway utilizing newly synthesized fatty acids could produce

508 at least some of the TAG in the HO line (Fig. 2, 3). The only Kennedy pathway
509 acyltransferase that was directly engineered into tobacco was AtDGAT1 (Vanhercke et
510 al., 2014). Therefore, TAG fatty acid composition is also dependent on the acyl
511 selectivity and substrate pools of the endogenous tobacco GPAT and LPAT. *In vitro*
512 assays did not produce TAG with microsomes from either the WT or the HO line (Fig.
513 4). This result may suggest that the four reactions of the Kennedy pathway in the HO
514 line are not associated together in the isolated microsomes for efficient shuttling of
515 substrates within the *in vitro* reactions. To further understand the path of acyl flux in WT
516 and HO leaves we utilized an *in vivo* labeling approach.

517 Multiple lines of evidence from the *in vivo* labeling results suggest a traditional
518 Kennedy pathway is not the major pathway of TAG synthesis in HO leaves. First, even
519 though fatty acids accumulate in HO TAG to levels that are 12-times that of PC (Fig.
520 2A), nascent fatty acids are incorporated into PC faster than into TAG (Fig. 5D).
521 Second, during the pulse-chase, fatty acids are redistributed predominantly from PC
522 into TAG (Fig. 9). Third, regiochemical analysis of *de novo* synthesized DAG indicated
523 an equal partitioning of labeled acyl chains at both *sn*-1 and *sn*-2 whereas TAG
524 contained nascent fatty acids only at *sn*-3 (Fig. 7). The regiochemical data indicates that
525 *de novo* DAG produced by Kennedy pathway GPAT/LPAT reactions (Fig. 1A) is not
526 directly used for TAG biosynthesis. In combination with the *in vitro* assay, the results
527 suggest that overexpressed AtDGAT1 does not produce a Kennedy pathway that
528 channels newly synthesized fatty acids directly into TAG.

529 The results in this study are most consistent with Fig. 1 option C which indicates
530 that a second pool of DAG (other than Kennedy pathway *de novo* DAG) is used for TAG
531 synthesis. It is not immediately clear how the second DAG pool is produced, it could be
532 derived from *de novo* DAG, or PC, or a combination of the two. The pulse-chase results
533 indicate that galactolipids, including MGDG, are not used for TAG production (Fig. 9).
534 Thus, the reported mechanisms that turn over chloroplast lipids to produce DAG for leaf
535 TAG under stress conditions (Vanhercke et al., 2019), are unlikely to be actively
536 contributing to TAG accumulation in HO tobacco leaves. Metabolic labeling with
537 [^{14}C]glycerol in developing oil seed tissues has suggested that a PC-derived DAG pool
538 is utilized for TAG synthesis (Bates et al., 2009; Bates and Browse, 2011; Yang et al.,

2017). The current [^{14}C]acetate acyl labeling cannot directly confirm a PC-derived DAG pool, but the acyl labeling results are consistent with the previous studies. It is also possible that immediately synthesized *de novo* DAG may feed into a larger and more slow turnover DAG pool such as in oil bodies where AtDGAT1 may co-localize with oleosin proteins. DAG can phase partition into oil bodies (Slack et al., 1980; Kuerschner et al., 2008). Thus, if the rapidly labeled *de novo* DAG mixes with a larger unlabeled pool in the oil body it would slow the apparent flux of the *sn*-1/2 labeled *de novo* DAG into TAG relative to the *sn*-3 TAG labeling of the total mixed DAG pool.

Both WT and HO leaf acyl fluxes are dominated by phosphatidylcholine acyl editing

In both WT and HO leaves, most newly synthesized fatty acids are immediately incorporated into PC (Fig. 5). The difference in stereochemical incorporation of newly synthesized fatty acid in DAG and PC (Fig. 7) indicates there is no DAG-PC precursor-product relationship at the earliest labeling time points. PC labeling as a percent of ER lipid labeling (Fig. 6) at 3 min indicates that PC is 94.9 ± 1.5% of the total labeled ER lipids in the WT, and 70 ± 4% in the HO line. The simplest interpretation of this result is a shift in acyl flux away from PC acyl editing in the HO line for direct incorporation of nascent fatty acids into the *sn*-3 position of TAG (Fig. 7). However, the production of TAG at heightened levels requires three acyl chains, of which a substantial percentage are PUFAs. Acyl editing is a constant exchange of acyl groups in PC with the acyl-CoA pool to accommodate desaturation. Thus, if the rate of acyl editing was increased in the HO line, a proportion of the labeled fatty acids initially incorporated into PC at time zero would be redistributed back to the acyl-CoA pool for use by AtDGAT1 to produce TAG within 3 minutes. This concept is supported with linear regression data used to determine labeling rates in Table 1. Extrapolating back to time zero the x-intercepts of PC are 0.91 for WT, and 0.93 for HO. For TAG the x-intercepts are 2.5 for WT, and 2.4 for HO. The similar labeling lag times between the WT and the HO line suggest a common path of nascent fatty acid incorporation into ER lipids, though at a higher rate (1.7-fold) for the HO line (Fig. 6). Thus, the rate of acyl editing in the HO line was

570 enhanced by the same amount (i.e. 1.7-fold) to accommodate the increased rate of fatty
571 acid export from the plastid, and PC is the first product of nascent fatty acid
572 incorporation into glycerolipids of the eukaryotic pathway.

573 The stereochemical distribution of labeled fatty acids in PC indicates that the
574 initial incorporation of nascent fatty acids into PC can occur at both positions but with an
575 approximately 2-fold preference for *sn*-2 (Fig. 7). The slightly higher PC *sn*-2 labeling in
576 the HO line suggests that the increase in PC acyl editing favors *sn*-2 over *sn*-1
577 positions. Therefore, acyl flux around the PC acyl editing cycle (Figure 1, option B) is
578 the dominate acyl flux reaction in both WT and HO tobacco, similar to what has been
579 demonstrated in leaves of pea, Arabidopsis, and rapeseed (Williams et al., 2000; Bates
580 et al., 2007; Karki et al., 2019), and developing seeds of soybean, camelina, and
581 Arabidopsis (Bates et al., 2009; Bates and Browse, 2011; Yang et al., 2017). Both PC
582 acyl chains are the major extra-plastidic sites for fatty acid desaturation (Sperling and
583 Heinz, 1993; Sperling et al., 1993), therefore 18:1 flux through PC acyl editing at both
584 *sn*-1 and *sn*-2 likely contributes to a PUFA containing acyl-CoA pool that leads to the
585 incorporation of PUFA in TAG of HO leaves. The decrease in the PC desaturation index
586 (Fig. 3C) is also consistent with an increased rate of acyl flux through PC, because
587 membrane lipid desaturation is dependent on both the rate of desaturation and the rate
588 of acyl flux through the membrane lipid. Increases in the fatty acid synthesis rate have
589 been demonstrated to increase 18:1 and decrease PUFA content of membrane lipids
590 (Maatta et al., 2012; Meï et al., 2015; Botella et al., 2016). Considering that the
591 engineering of a very large pull of acyl chains into TAG in the HO line only increases PC
592 acyl editing instead of drawing acyl chains away from it, PC acyl editing may be
593 considered a key part of fatty acid export from the plastid into the eukaryotic pathway.

594 Interestingly, both the [^{14}C]acetate continuous pulse and the pulse-chase
595 experiments produced similar initial labeling in lipids for the WT and the HO line (Fig. 6,
596 Fig. 8), but the pulse-chase experiment showed a more dramatic labeling in the
597 immediate chase period in the HO line relative to the WT (Fig. 8). Such a description of
598 initial labeling is consistent with hypothesized transport of acyl chains out of the
599 chloroplast and directly into PC that subverts the large bulk acyl-CoA pool as has been
600 previously documented through bulk pool kinetic measurements with time course

601 labeling experiments (Tjellström et al., 2012; Allen, 2016) and isotopically labeled
602 mutant analysis (Bates et al., 2009; Karki et al., 2019), and is likely part of the acyl
603 editing mechanism where rapid labeling in PC from [^{14}C]acetate was initially observed
604 (Bates et al., 2007; Bates et al., 2009). During the pulse-chase experiment, it may be
605 that the bulk acyl-CoA pool in the HO line is larger and becomes more labeled over the
606 duration of the pulse by enhanced flux through the acyl editing cycle, and therefore can
607 make a greater contribution to total lipid labeling during the initial phase of chase.
608
609 **Reduced prokaryotic pathway and altered redistribution of acyl chains from PC to**
610 **other lipids in the HO line**
611
612 Engineering the accumulation of TAG in the HO line reduced the steady-state
613 accumulation of chloroplast localized galactolipids by approximately 24% (Fig. 2). Total
614 MGDG content in the HO line was reduced ~19%, and the proportion of prokaryotic
615 pathway produced MGDG was reduced ~40% (Supplemental Fig. S1). DGDG is
616 produced mostly by eukaryotic pathway derived substrates, and total DGDG levels were
617 reduced by ~32% in the HO line as compared to the WT. Therefore, the mass
618 accumulation of galactolipids indicates that TAG accumulation in the HO line negatively
619 affects galactolipid production through both the prokaryotic and eukaryotic pathways.
620 The reductions in galactolipid levels in the HO line could be due to reduced
621 synthesis, increased turnover, or both which cannot be determined from the
622 quantification of steady-state lipid levels; but are reflected in time course-based acyl flux
623 experiments. At short time points [^{14}C]acetate labeling of nascent fatty acid flux into
624 MGDG represents predominantly prokaryotic MGDG, which is reduced almost 5-fold in
625 the HO line (Fig. 5, Tables 1-2). Therefore, the reduction in prokaryotic MGDG
626 accumulation is primarily due to reduced synthesis. It's also possible that homeostatic
627 turnover of galactolipids was reduced to allow higher accumulation of MGDG than
628 would be expected from the low rates of synthesis. To track the PC-MGDG precursor-
629 product relationship of eukaryotic MGDG synthesis, we used pulse-chase analyses with
630 longer time points. The [^{14}C]acetate pulse-chase labeling indicated that the
631 redistribution of acyl groups from PC in the HO line was predominantly into TAG with

reduced flux into eukaryotic MGDG synthesis as well as other lipids when compared to the WT (Figure 9, Table 3). As there was no reduction in total ^{14}C-MGDG accumulation during the chase period in the HO line, the reduced eukaryotic MGDG accumulation was due to reduced redistribution of acyl groups from PC to MGDG through the eukaryotic pathway. Thus there is no evidence to suggest enhanced galactolipid turnover in the HO line.

There are likely multiple alterations in enzymatic activity that led to the redistribution of acyl flux through the lipid metabolic network in the HO line. From the acyl flux analysis, we can propose several related hypotheses for future studies. First, the massive increase in fatty acid accumulation in TAG of the HO line combined with the reduced prokaryotic pathway are likely both related to an increase in acyl-ACP thioesterase activity, which removes the substrate for the prokaryotic pathway and initiates fatty acid export from the chloroplast (Bates et al., 2013; Li-Beisson et al., 2013). The gene expression of both thioesterases FATA and FATB were up regulated in the HO line (Vanhercke et al., 2017). The reduced prokaryotic pathway flux (Fig 5, 9, Tables 2-3), combined with the reduced rates of MGDG desaturation in the HO line (Supplemental Figs. S5-S6) also suggest a possible general down regulation of prokaryotic pathway enzymatic activity.

Second, within the eukaryotic pathway 1/3 of the fatty acids in TAG are incorporated into TAG directly from the acyl-CoA pool by the acyltransferase activity of the overexpressed AtDGAT1. In the WT the exchange of fatty acids from PC into the acyl-CoA pool would be mostly used for *de novo* glycerolipid synthesis that would produce the molecular species of PC used for eukaryotic galactolipid synthesis (Karki et al., 2019). Therefore, the increased flux around the PC acyl editing cycle combined with enhanced DGAT activity in the HO line would draw acyl flux away from PC and into *sn*-3 TAG, and reduce the amount of fatty acids available for *de novo* PC and galactolipid synthesis.

Third, the reduction in eukaryotic galactolipid synthesis of the HO line may also be due to reduced turnover of PC to produce the PC-derived substrate for galactolipid synthesis, or the commandeering of that PC-derived substrate for TAG biosynthesis. The identity of the eukaryotic pathway substrate that is transferred from the ER to the

plastid is not clear, and leading candidates include PC, and PC-derived PA and/or DAG (Hurlock et al., 2014; LaBrant et al., 2018; Karki et al., 2019). If PC-derived DAG is the substrate that is transferred from the ER to the chloroplast for galactolipid synthesis, then the overexpressed AtDGAT1 may compete for the PC-derived DAG substrate in the ER and reduce its transfer to the chloroplast for eukaryotic galactolipid synthesis. However, if PA is the PC-derived species that is transferred to the chloroplast, then it would not be a substrate for AtDGAT1 activity unless PA phosphatase activity was also upregulated to convert PA to DAG. Our previous transcriptomics in the HO line indicated increased expression of two phospholipase D isoforms which could produce PA from PC, however an increase in PA phosphatase expression was not detected (Vanhercke et al., 2017). In Arabidopsis the *TRIGALACTOSYLDIACYLGLYCEROL 1* mutant (*tgd1*) or overexpression of (*PDAT1*) increases WT leaf TAG content from <0.1% of dry weight to ~0.5% and ~1% of dry weight, respectively. Mutation of PA phosphatase activity in the *PHOSPHATIDIC ACID HYDROLASE 1* and *2* double mutant (*pah1 pah2*) reduces this TAG accumulation in both the *tgd1* and *AtPDAT1* overexpression backgrounds suggesting that PA phosphatase activity may be involved in leaf TAG production (Fan et al., 2014). However, the *pah1 pah2* mutant has increased synthesis and double the accumulation of leaf PC and PE content (Eastmond et al., 2010). In WT Arabidopsis leaves PC and PE accumulate 5- to 10-fold more fatty acids than TAG (Fan et al., 2014), therefore the effect of the *pah1 pah2* double mutation on leaf TAG accumulation in the *tgd1* and *AtPDAT1* overexpression lines may be due to a shift in fatty acid allocation from TAG to ER membrane lipids, rather than a reduction in TAG biosynthetic capacity. Therefore, the previous results in Arabidopsis and our transcriptomics have not fully elucidated the role of PA phosphatases in leaf TAG production. In addition, our analysis of acyl fluxes alone could not confirm if the DAG pool for TAG synthesis was derived from PC or not. Therefore, further [^{14}C]glycerol labeling experiments to confirm if HO leaf TAG is derived from PC, combined with analysis of changes in PC lipase and PAP enzymatic activities would be beneficial to determining both the altered pathway fluxes in the HO line, as well as identifying the PC-derived substrate that is used for eukaryotic galactolipid synthesis.

The tobacco leaf acyl flux analysis suggests strategies to reduce PUFA accumulation in leaf oil

To reduce the PUFA content of oilseed crops, research has focused on reducing seed specific FATTY ACID DESATURASE 2 and 3 (FAD2 and FAD3) activity through mutations of isoforms mostly expressed in seeds but not vegetative tissue (Pham et al., 2010), or through seed specific RNA interference (Wood et al., 2018; Islam et al., 2019). The purpose of the seed specific reduction in desaturase activity is to increase the oleate content of the seed oil, but not effect leaf membrane lipid compositions in vegetative tissue. ER membrane based FAD2 activity is required for proper leaf membrane function, especially at low temperatures (Miquel et al., 1993). Due to the importance of leaf desaturases for vegetative growth, a similar reduction of desaturase activity would likely be counterproductive in a vegetative oil crop. The analysis of acyl fluxes in WT and HO tobacco leaves presented here indicate that fatty acid flux through the PC acyl editing cycle is the dominate reaction in the WT, and is enhanced at least 1.7-fold in the HO line. Because PC is the site for ER localized fatty acid desaturation this movement of acyl groups through PC contributes to accumulation of PUFA in HO leaf TAG. Therefore, an alternative strategy may be to alter acyl flux away from PC. In Arabidopsis The LYSOPHOSPHATIDYLCHOLINE ACYLTRANSFERASEs (LPCAT1, LPCAT2) are responsible for the direct incorporation of nascent fatty acids into PC through acyl editing in both leaves (Karki et al., 2019) and seeds (Bates et al., 2012). The *lpcat1 lpcat2* double mutant alters acyl flux such that nascent fatty acids are first esterified into glycerol lipids through the GPAT and LPAT reactions of the Kennedy pathway, rather than PC acyl editing (Bates et al., 2012; Karki et al., 2019). In seeds, this leads to an increase in the seed oil monounsaturated/polyunsaturated fatty acid ratio from 0.72 to 0.84. When reduced exchange of DAG in and out of PC of the PHOSPHATIDYLCHOLINE: DIACYLGLYCEROL CHOLINEPHOSPHOTRANSFERASE mutant *rod1* is combined with the *lpcat1 lpcat2* double mutant, the ratio is further increased to 3.95 in the *lpcat1 lpcat2 rod1* triple mutant (Bates et al., 2012). From our current analysis it was unclear if leaf TAG was produced from PC-derived DAG, but if PC-derived DAG also contributes to leaf TAG a similar approach reducing acyl editing

and PC-derived DAG production may be valuable to alter acyl flux around PC to increase the oleate content of leaf TAG while maintaining the PUFA content of membranes. Therefore, the acyl flux analysis presented here has improved our understanding of how leaf lipid metabolism responds to an increased push and pull of fatty acids into TAG, as well as provided new hypotheses on how to further enhance vegetative oil engineering.

In summary the analysis of acyl fluxes in WT and HO tobacco leaves indicate: (1) The push and pull leaf oil production in the HO line reduces acyl flux into the prokaryotic and enhances flux into the eukaryotic glycerolipid assembly pathways. (2) Fatty acids entering the eukaryotic pathway are first incorporated into PC through acyl editing in both the WT and the HO tobacco plants. (3) The high flux of nascent acyl groups directly into PC acyl editing, and the initial labeled TAG regiochemical analysis both indicate that a direct Kennedy pathway of TAG biosynthesis with nascent fatty acids is not occurring in HO leaves. (4) In HO leaves acyl groups are redistributed from PC mostly into TAG, rather than eukaryotic MGDG production as in the WT. (5) The enhanced flux of fatty acids into TAG combined with the reduced flux of fatty acids into both the prokaryotic and eukaryotic pathways of galactolipid synthesis reduced the steady-state accumulation of MGDG and DGDG. (6) The pulse-chase did not indicate TAG synthesis from galactolipid turnover. (7) Characterization of the high rates of PC acyl editing in the HO line suggests that limiting PC acyl editing may be a future engineering strategy to increase the monounsaturated fatty acid content of leaf derived biofuels.

METHODS

Plant growth

For lipid mass analysis and metabolic labeling experiments, WT and HO tobacco (*Nicotiana tabacum*) plants were grown in Percival E-41HO growth chambers set at 16/8 hours light/dark, 26/22°C, and fluorescent white light intensity at pot level across the chamber was 300-400 µmol photons m^{-2} s^{-1}. Pots were watered three times a week, with one watering replaced by Peters 20/20/20 NPK fertilizer at 0.97 g/L once a week. For microsomal assays, tobacco plants were grown in the glasshouse during summer condition at 24°C/18°C for 16 hr/8 hr light/dark.

Chemicals and supplies

Unless specified all chemicals were purchased from Fisher Scientific (www.fishersci.com), and solvents were at least HPLC grade. [^{14}C]acetate sodium salt 50 mCi/mmol (American Radiolabeled Chemicals, Inc. St. Louis, MO). Glass TLC plates: Analtech HL 250 µm, 20 x 20 cm. Liquid scintillation fluid: EcoScint Original (National Diagnostics, Atlanta, GA). Lipase from *Rhizomucor miehei* and Phospholipase A2 lipase from *Apis mellifera* (Sigma-Aldrich, St. Louis, MO).

Microsomal assays

Leaves were harvested from 66-day-old tobacco plants, and the microsomal proteins were prepared as described (Zhou et al., 2013). Protein content of the microsomal preparations was measured with BCA reagents (Pierce Chemical Company) with BSA as a standard. The enzyme assay was essentially done as described (Guan et al., 2014). Microsomal proteins (100 µg) were incubated at 30°C with gentle shaking in 0.1 M Tris buffer pH 7.2 containing 4 mM $MgCl_2$, 10 mg/ml BSA, 12.5 nmol of [^{14}C]glycerol-3-phosphate (8000 dpm/nmol) and 25 nmol 18:1-CoA in a final assay volume of 100 µL for 15 or 60 min. The assays were terminated by addition

781 of 250 µL of methanol/chloroform/acetic acid (50:50:1) (v/v/v), followed by extraction of
782 the lipids into a chloroform phase. The total lipids were separated on silica TLC plates
783 by developing with chloroform/methanol/acetic acid/water, 90:15:10:3 (v/v/v/v) to half-
784 way of the plate to separate the polar lipids. After air drying for a few minutes, the plates
785 were redeveloped with hexane/diethyl either/acetic acid, 70:30:1 (v/v/v) to separate the
786 neutral lipids. Radioactive labels of 1000 dpm were spotted three times on each plate as
787 reference, before exposing to a phosphor image screen for overnight. The radioactivity
788 of each band was quantified with Fujifilm FLA-5000 Phosphor Imager.
789
790 *Continuous pulse and pulse-chase [^{14}C]acetate metabolic labeling*
791
792 The continuous pulse metabolic labeling of WT and HO leaf disks was done for
793 3, 6, 10, 30, 120 minutes in triplicate, within 20 mM MES pH 5.5, 0.1X MS salts, 0.01%
794 Tween 20, and 1 mM [^{14}C]acetate. Procedure: 10 mm diameter leaf disks were
795 collected from multiple plants (two WT and three HO) randomized across all horizontal
796 leaves. For each time point replicate, 12 disks were collected directly into 10 mL
797 incubation media (without [^{14}C]acetate) in 100 mL beakers and placed in a 26°C water
798 bath under ~330 µmol photons m^{-2} s^{-1} white light with gentle shaking for 10 min to
799 equilibrate temperature. To start the labeling time course the media was removed and
800 replaced with 5 mL of incubation media with [^{14}C]acetate. At each time point the media
801 was removed and the 12 leaf disks were placed into 85°C 2.5 ml isopropanol, 0.01%
802 (w/v) butylated hydroxytoluene for 10 min to quench metabolism. Each replicate time
803 course for each plant line used three 5 ml aliquots of 1 mM [^{14}C]acetate labeling media.
804 The remaining [^{14}C]acetate media after the 6 min time point was used for the 120 min
805 labeling, and the remaining media from the 10 min time point was used for the 30 min
806 labeling. The remaining [^{14}C]acetate media from the 3 and 10/30 labeling time points
807 were mixed and used for the pulse-chase [^{14}C]acetate labeling.
808 For each of the triplicate pulse-chase labeling time courses, 24 leaf disks were
809 collected as described above and pulsed with [^{14}C]acetate labeling media independently
810 for 30 min. The ^{14}C media was removed and the disks were washed three times (10 ml
811 each) in media without [^{14}C]acetate and a final 10 mL media was added for chase

incubations. At each chase time point of 0, 2, 6, and 22 hours six leaf disks were collected from each time course incubation and quenched as described above.

Lipid extraction and lipid class TLC separations

Lipids were extracted from isopropanol quenched tissue following a previous method (Hara and Radin, 1978). After drying total extracts under N_2, lipids of each extract were dissolved in 0.5 ml toluene and aliquots were used for various analytical procedures. Total ^{14}C extracts were quantified by liquid scintillation counting on a Beckman Coulter LS 6500 liquid scintillation counter. Neutral lipids were separated on silica TLC plates in hexane/diethyl either/acetic acid, 70:30:1 (v/v/v). Polar lipids were resolved with toluene/acetone/water (30/91/7, v/v/v) on silica TLC plates pre-treated with 0.15 M ammonium sulfate and baked at 120°C for 3 hours prior to loading lipids. Lipid classes were identified based on co-migration with standards. Relative radioactivity of lipids separated by TLC was measured by phosphor imaging on a GE Typhoon FLA7000, and ImageQuant analysis software.

Leaf lipid mass analysis

Leaf lipids extracted from 86-day-old plants were separated by TLC as described above, and stained with 0.05% primulin in acetone/water 80:20 (v/v) and visualized under UV light. Scraped bands were transmethylated along with a 17:0 TAG internal standard of fatty acid methyl esters (FAMEs) in 2.5% (v/v) sulfuric acid in methanol at 80°C for 1 hr. FAMEs were collected into hexane by adding hexane and 0.88% (w/v) NaCl to force a phase separation. FAMEs were separated and quantified by gas chromatography with flame ionization detection on a Restek Stabilwax column: 30 m, 0.25 ID, 0.25 µm film thickness.

Regiochemical analysis of DAG, PC, and TAG

Total lipids extracted as described above from the WT and the HO line were co-loaded with 30 µg PC and 30 µg DAG. For the WT, 30 µg TAG was also co-loaded. Polar lipid and neutral lipid TLC and primulin staining was performed as described above. PC bands were scrapped off and eluted with chloroform/methanol/acetic acid (5:5:1, v/v/v). Partial digestion of PC was performed with bee venom (*Apis mellifera*) phospholipase PLA_2 (Sigma) (Bates et al., 2007). The digested products were separated by TLC in chloroform/methanol/acetic acid/water 50:30:8:4 (v/v/v/v). Regiochemical analysis of neutral lipids were performed as described (Cahoon et al., 2006). DAG and TAG were digested with 0.2 ml of the *Rhizomucor meihei* lipase (Sigma) for 30 and 60 min respectively. Digested products were separated by TLC in hexane/diethyl ether/acetic acid (35:70:1, v/v/v). Lipid standards were stained with iodine vapor and marked with ^{14}C. Identification of unknowns was based on co-migration with standards. Radioactivity was quantified by using phosphor imaging as described above.

Analysis of [^{14}C]acetate labeled MGDG molecular species

MGDG was isolated by normal phase HPLC on an Agilent 1260 Infinity II (quaternary pump, autosampler, column thermostat, DAD set to 210 nm, fraction collector, running OpenLAB CDS Version C.01.09). The method is an adaption of (Kotapati and Bates, 2018), with modifications as follows: injection volume 5-15 µL in toluene; flow rate 1 ml/min; mobile phases (A: 2-Propanol, B: hexanes, C: Methanol, D:25 mM triethylamine + 25 mM Formic acid (pH 4.1)). Linear gradients between steps from: 0 min 19.3%A/80%B/0.5%C/0.20%D; 3 min 73.6%A/25%B/1%C/0.4%D; 6 min 87.5%A/10%B/1.5%C/1%D; 15 min 65%A/0%B/25%C/10%D; held for 3 min; 20 min 100%A; held for 3 min; 24 min is the starting composition, and equilibration between samples is 10 min. MGDG was collected between 5.3 and 6.2 min. MGDG molecular species were separated by HPLC on a Thermo Scientific Accucore C18 column (150 mm x 3mm; 2.6 µ particle size), according to (Yamauchi et al., 1982) except that the flow rate was 0.35 ml/min for 35 minutes. Vial sampler was maintained at 20°C and the column compartment at 35°C. Samples were injected in 8-15 µL methanol and

contained 5000-20000 CPM. To measure radioactivity the column eluent flowed into a LabLogic β-Ram 6 flow liquid scintillation detector, flow cell volume set at 300 µL, eluant:scintillation cocktail (LabLogic FloLogic-U) ratio was 1:3, with a residence time of 12.9 s. Laura 6.0.1.40 software was used to acquire and process the ^{14}C data. To confirm the identity of labeled molecular species, each fraction was collected, converted to FAME as above, and separated by argentation TLC as in (Bates et al., 2009).

Data analysis

All calculations from raw data were done in Microsoft Excel. Graphing and statistical analysis done with GraphPad Prism version 7.05.

Accession Numbers

AtWRI1, AT3G54320; AtDGAT1, AT2G19450; SiOLEOSIN; EU999158; AtFAD2, AT3G12120; AtFAD3, AT2G29980; AtLPCAT1, AT1G12640; AtLPCAT2, AT1G63050; AtPAH1, AT3G09560; AtPAH2, AT5G42870; AtPDAT1, AT5G13640; AtROD1, AT3G15820; AtTGD1, AT1G19800.

Supplemental Data

Supplemental Figure S1. Stereochemical fatty acid composition of MGDG and DGDG from WT and HO leaves.

Supplemental Figure S2. Total incorporation of [^{14}C]acetate into WT and HO leaves.

Supplemental Figure S3. Initial incorporation of nascent [^{14}C]acetate labeled fattyacids into lipids, non-normalized.

Supplemental Figure S4. Example of ^{14}C-MGDG molecular species analysis.

Supplemental Figure S5. Labeled MGDG molecular species from 30 and 120 minute continuous [^{14}C]acetate labeling.

Supplemental Figure S6. Labeled MGDG molecular species from 0 and 22 hours pulse-chase [^{14}C]acetate labeling.

ACKNOWLEDGEMENTS

We thank Bei Dong for technical support.

TABLES

	PC	PE	PG	MGDG	DGDG	DAG	TAG
WT	18.59 ± 2.97	1.53 ± 0.17	0.31 ± 0.004	16.49 ± 1.79	0.28 ± 0.0001	2.08 ± 0.35	0.14 ± 0.01
HO	17.2 ± 1.7	1.04 ± 0.13	*0.16 ± 0.02	*3.36 ± 0.59	*0.11 ± 0.01	1.57 ± 0.37	*16.68 ± 2.83
p-value	0.7234	0.1444	0.0263	0.0199	0.0075	0.4212	0.0281
F.C.			-1.9	-4.9	-2.5		119.1

Table 1. Initial rates of nascent fatty acid incorporation into individual lipid classes.

Rates in DPM μchlorophyll^{-1} min^{-1} are the slope best fit ± SE from the linear regression of the first 10 minutes of [^{14}C]acetate labeling from Fig. 5. The p-values indicate if the slopes are significantly different (p-value < 0.05), those that are significant are marked with an asterisk. The fold change (F.C.) for lipids with significantly different rates are indicated.

Samples:	WT 30 min	HO 30 min	HO % of WT DPM	WT 120 min	HO 120 min	HO % of WT DPM
Ave. total DPM/μg chl	335.2	86.7		2066.4	646.6	
Eukaryotic proportion	**9.6%**	**20.9%**		**11.4%**	**25%**	
DPM/μg chl	32.2	18.1	56.3%	234.5	161.7	69%
Prokaryotic proportion	**90.4%**	**79.1%**		**88.6%**	**75%**	
DPM/μg chl	303.0	68.2	22.6%	1831.9	484.6	26.5%

Table 2. Acyl flux into eukaryotic and prokaryotic molecular species of MGDG

The average total MGDG DPM/μg chl at 30 and 120 min is from Fig. 5. The proportion of eukaryotic and prokaryotic molecular species are from Supplemental Figure S5. The DPM/μg chl of eukaryotic and prokaryotic MGDG molecular species are calculated from

924 the total label and the relative proportion of each. The "HO % of WT DPM" is the
925 amount of HO eukaryotic or prokaryotic MGDG as compared to the WT at each time
926 point.
927
928
929
930

Samples:	WT 0 hr	WT 22 hr	0-22 hr F.C.	HO 0 hr	HO 22 hr	0-22 hr F.C.
Eukaryotic proportion	12.8%	38.6%	3.0	20.4%	31.5%	1.5
Prokaryotic proportion	87.2%	61.4%	0.7	79.5%	68.5%	0.86

931

932 **Table 3. Change in MGDG eukaryotic and prokaryotic molecular species over the**
933 **[^{14}C]acetate pulse-chase.** The proportion of eukaryotic and prokaryotic molecular
934 species are from Supplemental Figure S6. F.C., fold-change.
935

936 **Figure Legends**
937

938 **Figure 1. Model of leaf lipid pathways and hypotheses for acyl flux into TAG.**
939 Plastid localized fatty acid synthesis (F.A.S.) and chloroplast localized prokaryotic
940 pathway are in the green box. All other reactions represent extra-plastidial metabolism.
941 Filled arrowheads represent flux of the glycerol backbone, open arrowheads represent
942 acyl transfer reactions. Dashed lines and boxes represent uncertainty in acyl flux in HO
943 tobacco lines, and large blue letters represent 3 hypotheses for altered acyl flux in HO
944 tobacco lines: A, the use of *de novo* DAG by AtDGAT1 for a Kennedy pathway TAG
945 synthesis; B, uncertain quantitative flux through acyl editing that affects incorporation of
946 PC-modified fatty acids in TAG; C, the use of a membrane lipid derived DAG by
947 AtDGAT1 for TAG synthesis. Abbreviations: DAG, diacylglycerol; DGDG,
948 digalactosyldiacylglycerol; G3P, glycerol-3-phosphate; LPA, lysophosphatidic acid;
949 MGDG; monogalactosyldiacylglycerol; PA, phosphatidic acid; PC, phosphatidylcholine;
950 PE, phosphatidylethanolamine; PG, phosphatidylglycerol; TAG, triacylglycerol.
951

Figure 2. Accumulation of lipids in WT and HO leaves.

The abundance of polar membrane lipids and neutral lipids in leaves of 86-day-old plants. A, mass abundance of each lipid. B, ratio of mass abundance of lipid to PC. WT, blue. HO, red. Data is average ± SEM for 3-4 replicates. Significant differences in the HO line from the WT (Student's *t*-test, p-value < 0.05) are marked with an asterisk. Abbreviations: DAG, diacylglycerol; DGDG, digalactosyldiacylglycerol; MGDG; monogalactosyldiacylglycerol; PC, phosphatidylcholine; PE, phosphatidylethanolamine; PG, phosphatidylglycerol; PI, phosphatidylinositol; PS, phosphatidylserine; TAG, triacylglycerol.

Figure 3. Fatty acid composition of WT and HO leaf lipids.

Weight percent fatty acid composition of lipid classes isolated from leaves of 86-day-old plants. A, total leaf extract. B, TAG. C, PC. D, MGDG. Abbreviations as in text. WT, blue. HO, red. Data is average ± SEM for 3-4 replicates. Significant differences in the HO line from the WT (Student's *t*-test, p-value < 0.05) are marked with an asterisk. Abbreviations: PC, phosphatidylcholine; MGDG, monogalactosyldiacylglycerol; TAG, fatty acids, # carbons: # double bonds, d#, delta double bond position.

Figure 4. In vitro assay of the Kennedy pathway in leaf microsomes.

Assay conditions: 100 ug of leaf microsomal protein, 12.5 nmole [^{14}C]G3P + 25 nmole of 18:1-CoA, incubated for 15 or 60 min. For each line and assay length, data is the average and SEM of 3 replicates. Abbreviations: DAG, diacylglycerol; LPA, lysophosphatidic acid; PA, phosphatidic acid; MAG, monoacylglycerol; TAG, triacylglycerol.

Figure 5. Initial incorporation of nascent [^{14}C]acetate labeled fatty acids into lipids.

A-B, major labeled lipids from continuous [^{14}C]acetate labeling for 3-120 min in leaf disks of 66-day-old plants of the WT and the HO line. C-D, an expanded view of the 0-35 min portion of A & B. All data points are average and SEM of 3 biological replicates. Abbreviations: DAG, diacylglycerol; DGDG, digalactosyldiacylglycerol; MGDG;

monogalactosyldiacylglycerol; PC, phosphatidylcholine; PE, phosphatidylethanolamine; PG, phosphatidylglycerol; TAG, triacylglycerol; DPM, disintegrations per minute; chl, chlorophyll.

Figure 6. Relative incorporation of nascent fatty acids into the eukaryotic and prokaryotic pathways of WT and HO leaves. A, the WT. B, the HO line. The endoplasmic reticulum (ER) localized lipids (PC, PE, TAG) and the plastid localized lipids (PG, MDGD, DGDG) from Fig. 5 were added together, and the ratio of the two. DAG was not included because it can be localized to multiple compartments. All data points are average and SEM of 3 biological replicates. Abbreviations: DPM, disintegrations per minute; chl, chlorophyll.

Figure 7. Regiochemical analysis of initial incorporation of nascent [^{14}C]acetate labeled fatty acids into DAG, PC, and TAG. A-B, TAG lipase digestion of DAG from the WT and the HO line. C-D, phospholipase A_2 digestion of PC from the WT and the HO lines. E-F, TAG lipase digestion of TAG from the WT and the HO line. All data points are average and SEM of 3 biological replicates. In A-D, statistical significance of the HO line from the WT (Student's *t*-test, p-value < 0.05) is marked with an asterisk at each data point. Abbreviations: DAG, diacylglycerol; FFA, free fatty acid; MAG, monoacylglycerol; PC, phosphatidylcholine; TAG, triacylglycerol.

Figure 8. Pulse-Chase [^{14}C]acetate accumulation in lipids of the WT and the HO line. In all panels the pulse starts at -0.5 hours, and the chase starts at 0 hours. The leaves of 73-day-old plants were used for both plants. A-B, the WT and the HO line demonstrating the total ^{14}C incorporated into the lipid extract; the endoplasmic reticulum (ER) localized lipids (PC, PE, TAG) and the plastid localized lipids (PG, MDGD, DGDG) were added together, and the ratio of the two. DAG was not included because it can be localized to multiple compartments. All data points are average and SEM of 3 biological replicates. Abbreviations: DPM, disintegrations per minute; chl, chlorophyll.

Figure 9. Pulse-Chase [^{14}C]acetate labeling of acyl flux through the lipid metabolic network. In all panels the pulse starts at -0.5 hours, and the chase starts at 0 hours. The leaves of 73-day-old plants were used for both plants. A-B, accumulation of individual radiolabeled lipids as DPM/µg chlorophyll from the total labeled samples in Fig. 8. C-D, the labeled lipids in A-B, represented as a percentage of the sum. All data points are average and SEM of 3 biological replicates. Abbreviations: DAG, diacylglycerol; DGDG, digalactosyldiacylglycerol; MGDG; monogalactosyldiacylglycerol; PC, phosphatidylcholine; PE, phosphatidylethanolamine; PG, phosphatidylglycerol; TAG, triacylglycerol; DPM, disintegrations per minute; chl, chlorophyll.

Parsed Citations

Allen DK (2016) Assessing compartmentalized flux in lipid metabolism with isotopes. Biochimica et Biophysica Acta (BBA) - Molecular and Cell Biology of Lipids 1861: 1226-1242

Pubmed: Author and Title
Google Scholar: Author Only Title Only Author and Title

Allen DK (2016) Quantifying plant phenotypes with isotopic labeling & metabolic flux analysis. Current opinion in biotechnology 37: 45-52

Pubmed: Author and Title
Google Scholar: Author Only Title Only Author and Title

Allen DK, Bates PD, Tjellström H (2015) Tracking the metabolic pulse of plant lipid production with isotopic labeling and flux analyses: Past, present and future. Progress in Lipid Research 58: 97-120

Pubmed: Author and Title
Google Scholar: Author Only Title Only Author and Title

Arisz SA, Heo J-Y, Koevoets IT, Zhao T, van Egmond P, Meyer J, Zeng W, Niu X, Wang B, Mitchell-Olds T, Schranz ME, Testerink C (2018) Diacylglycerol acyltransferase 1 contributes to freezing tolerance. Plant Physiology 177: 1410-1424

Pubmed: Author and Title
Google Scholar: Author Only Title Only Author and Title

Bafor M, Smith MA, Jonsson L, Stobart K, Stymne S (1991) Ricinoleic acid biosynthesis and triacylglycerol assembly in microsomal preparations from developing castor-bean (Ricinus-communis) endosperm. Biochemical Journal 280: 507-514

Pubmed: Author and Title
Google Scholar: Author Only Title Only Author and Title

Barron EJ, Stumpf PK (1962) Fat metabolism in higher plants. XIX. The biosynthesis of triglycerides by avocado-mesocarp enzymes. Biochim Biophys Acta 60: 329-337

Pubmed: Author and Title
Google Scholar: Author Only Title Only Author and Title

Bates PD (2016) Understanding the control of acyl flux through the lipid metabolic network of plant oil biosynthesis. Biochimica et Biophysica Acta (BBA) - Molecular and Cell Biology of Lipids 1861: 1214-1225

Pubmed: Author and Title
Google Scholar: Author Only Title Only Author and Title

Bates PD, Browse J (2011) The pathway of triacylglycerol synthesis through phosphatidylcholine in Arabidopsis produces a bottleneck for the accumulation of unusual fatty acids in transgenic seeds. Plant Journal 68: 387-399

Pubmed: Author and Title
Google Scholar: Author Only Title Only Author and Title

Bates PD, Browse J (2012) The significance of different diacylgycerol synthesis pathways on plant oil composition and bioengineering. Front Plant Sci 3: 147

Pubmed: Author and Title
Google Scholar: Author Only Title Only Author and Title

Bates PD, Durrett TP, Ohlrogge JB, Pollard M (2009) Analysis of Acyl Fluxes through Multiple Pathways of Triacylglycerol Synthesis in Developing Soybean Embryos. Plant Physiology 150: 55-72

Pubmed: Author and Title
Google Scholar: Author Only Title Only Author and Title

Bates PD, Fatihi A, Snapp AR, Carlsson AS, Browse J, Lu C (2012) Acyl editing and headgroup exchange are the major mechanisms that direct polyunsaturated fatty acid flux into triacylglycerols. Plant Physiology 160: 1530-1539

Pubmed: Author and Title
Google Scholar: Author Only Title Only Author and Title

Bates PD, Ohlrogge JB, Pollard M (2007) Incorporation of Newly Synthesized Fatty Acids into Cytosolic Glycerolipids in Pea Leaves Occurs via Acyl Editing. Journal of Biological Chemistry 282: 31206-31216

Pubmed: Author and Title
Google Scholar: Author Only Title Only Author and Title

Bates PD, Stymne S, Ohlrogge J (2013) Biochemical pathways in seed oil synthesis. Current Opinion in Plant Biology 16: 358-364

Pubmed: Author and Title
Google Scholar: Author Only Title Only Author and Title

Botella C, Sautron E, Boudiere L, Michaud M, Dubots E, Yamaryo-Botté Y, Albrieux C, Marechal E, Block MA, Jouhet J (2016) ALA10, a Phospholipid Flippase, Controls FAD2/FAD3 Desaturation of Phosphatidylcholine in the ER and Affects Chloroplast Lipid Composition in Arabidopsis thaliana. Plant Physiology 170: 1300-1314

Pubmed: Author and Title
Google Scholar: Author Only Title Only Author and Title

Browse J, Warwick N, Somerville CR, Slack CR (1986) Fluxes through the prokaryotic and eukaryotic pathways of lipid-synthesis in the 16:3 plant Arabidopsis-thaliana. Biochemical Journal 235: 25-31

Pubmed: Author and Title
Google Scholar: Author Only Title Only Author and Title

Cahoon EB, Dietrich CR, Meyer K, Damude HG, Dyer JM, Kinney AJ (2006) Conjugated fatty acids accumulate to high levels in phospholipids of metabolically engineered soybean and Arabidopsis seeds. Phytochemistry 67: 1166-1176
Pubmed: Author and Title
Google Scholar: Author Only Title Only Author and Title

Carlsson AS, Yilmaz JL, Green AG, Stymne S, Hofvander P (2011) Replacing fossil oil with fresh oil - with what and for what? Eur J Lipid Sci Technol 113: 812-831
Pubmed: Author and Title
Google Scholar: Author Only Title Only Author and Title

Cernac A, Benning C (2004) WRINKLED1 encodes an AP2/EREB domain protein involved in the control of storage compound biosynthesis in Arabidopsis. Plant J 40: 575 - 585
Pubmed: Author and Title
Google Scholar: Author Only Title Only Author and Title

Durrett TP, Benning C, Ohlrogge J (2008) Plant triacylglycerols as feedstocks for the production of biofuels. The Plant Journal 54: 593-607
Pubmed: Author and Title
Google Scholar: Author Only Title Only Author and Title

Eastmond PJ, Quettier A-L, Kroon JTM, Craddock C, Adams N, Slabas AR (2010) PHOSPHATIDIC ACID PHOSPHOHYDROLASE1 and 2 Regulate Phospholipid Synthesis at the Endoplasmic Reticulum in Arabidopsis. The Plant Cell Online 22: 2796-2811
Pubmed: Author and Title
Google Scholar: Author Only Title Only Author and Title

Fan J, Yan C, Roston R, Shanklin J, Xu C (2014) Arabidopsis Lipins, PDAT1 Acyltransferase, and SDP1 Triacylglycerol Lipase Synergistically Direct Fatty Acids toward beta-Oxidation, Thereby Maintaining Membrane Lipid Homeostasis. Plant Cell 26: 4119-4134
Pubmed: Author and Title
Google Scholar: Author Only Title Only Author and Title

Fernie AR, Stitt M (2012) On the discordance of metabolomics with proteomics and transcriptomics: coping with increasing complexity in logic, chemistry, and network interactions scientific correspondence. Plant Physiology 158: 1139-1145
Pubmed: Author and Title
Google Scholar: Author Only Title Only Author and Title

Focks N, Benning C (1998) wrinkled1: A novel, low-seed-oil mutant of Arabidopsis with a deficiency in the seed-specific regulation of carbohydrate metabolism. Plant Physiology 118: 91-101
Pubmed: Author and Title
Google Scholar: Author Only Title Only Author and Title

Frentzen M, Heinz E, McKeon TA, Stumpf PK (1983) Specificities and Selectivities of Glycerol-3-Phosphate Acyltransferase and Monoacylglycerol-3-Phosphate Acyltransferase from Pea and Spinach Chloroplasts. European Journal of Biochemistry 129: 629-636
Pubmed: Author and Title
Google Scholar: Author Only Title Only Author and Title

Guan R, Lager I, Li X, Stymne S, Zhu L-H (2014) Bottlenecks in erucic acid accumulation in genetically engineered ultrahigh erucic acid Crambe abyssinica. Plant Biotechnology Journal 12: 193-203
Pubmed: Author and Title
Google Scholar: Author Only Title Only Author and Title

Hajduch M, Hearne LB, Miernyk JA, Casteel JE, Joshi T, Agrawal GK, Song Z, Zhou M, Xu D, Thelen JJ (2010) Systems analysis of seed filling in Arabidopsis: using general linear modeling to assess concordance of transcript and protein expression. Plant physiology 152: 2078-2087
Pubmed: Author and Title
Google Scholar: Author Only Title Only Author and Title

Hara A, Radin NS (1978) Lipid extraction of tissues with a low-toxicity solvent. Analytical Biochemistry 90: 420-426
Pubmed: Author and Title
Google Scholar: Author Only Title Only Author and Title

Holzl G, Dormann P (2019) Chloroplast Lipids and Their Biosynthesis. Annu Rev Plant Biol 70: 51-81
Pubmed: Author and Title
Google Scholar: Author Only Title Only Author and Title

Hurlock AK, Roston RL, Wang K, Benning C (2014) Lipid Trafficking in Plant Cells. Traffic 15: 915-932
Pubmed: Author and Title
Google Scholar: Author Only Title Only Author and Title

Islam N, Bates PD, Maria John KM, Krishnan HB, Z JZ, Luthria DL, Natarajan SS (2019) Quantitative Proteomic Analysis of Low Linolenic Acid Transgenic Soybean Reveals Perturbations of Fatty Acid Metabolic Pathways. Proteomics 19: e1800379
Pubmed: Author and Title
Google Scholar: Author Only Title Only Author and Title

Karki N, Johnson BS, Bates PD (2019) Metabolically distinct pools of phosphatidylcholine are involved in trafficking of fatty acids out of and into the chloroplast for membrane production. The Plant Cell: 31: 2768-2788
Pubmed: Author and Title
Google Scholar: Author Only Title Only Author and Title

Katavic V, Reed DW, Taylor DC, Giblin EM, Barton DL, Zou JT, Mackenzie SL, Covello PS, Kunst L (1995) Alteration of seed fatty-acid composition by an ethyl methanesulfonate-induced mutation in Arabidopsis-thaliana affecting diacylglycerol acyltransferase activity. Plant Physiology 108: 399-409
Pubmed: Author and Title
Google Scholar: Author Only Title Only Author and Title

Kelly AA, Dormann P (2004) Green light for galactolipid trafficking. Curr Opin Plant Biol 7: 262-269
Pubmed: Author and Title
Google Scholar: Author Only Title Only Author and Title

Kotapati HK, Bates PD (2018) A normal phase high performance liquid chromatography method for the separation of hydroxy and non-hydroxy neutral lipid classes compatible with ultraviolet and in-line liquid scintillation detection of radioisotopes. Journal of Chromatography B 1102-1103: 52-59
Pubmed: Author and Title
Google Scholar: Author Only Title Only Author and Title

Kuerschner L, Moessinger C, Thiele C (2008) Imaging of lipid biosynthesis: how a neutral lipid enters lipid droplets. Traffic 9: 338-352
Pubmed: Author and Title
Google Scholar: Author Only Title Only Author and Title

LaBrant E, Barnes AC, Roston RL (2018) Lipid transport required to make lipids of photosynthetic membranes. Photosynthesis Research 138: 345-360
Pubmed: Author and Title
Google Scholar: Author Only Title Only Author and Title

Li-Beisson Y, Shorrosh B, Beisson F, Andersson MX, Arondel V, Bates PD, Baud S, Bird D, DeBono A, Durrett TP, Franke RB, Graham IA, Katayama K, Kelly AA, Larson T, Markham JE, Miquel M, Molina I, Nishida I, Rowland O, Samuels L, Schmid KM, Wada H, Welti R, Xu C, Zallot R, Ohlrogge J (2013) Acyl-Lipid Metabolism. the Arabidopsis Book 11: e0161
Pubmed: Author and Title
Google Scholar: Author Only Title Only Author and Title

Li-Beisson Y, Shorrosh B, Beisson F, Andersson MX, Arondel V, Bates PD, Baud S, Bird D, Debono A, Durrett TP, Franke RB, Graham IA, Katayama K, Kelly AA, Larson T, Markham JE, Miquel M, Molina I, Nishida I, Rowland O, Samuels L, Schmid KM, Wada H, Welti R, Xu C, Zallot R, Ohlrogge J (2013) Acyl-lipid metabolism. Arabidopsis Book 11: e0161
Pubmed: Author and Title
Google Scholar: Author Only Title Only Author and Title

Lu CF, Napier JA, Clemente TE, Cahoon EB (2011) New frontiers in oilseed biotechnology: meeting the global demand for vegetable oils for food, feed, biofuel, and industrial applications. Current Opinion in Biotechnology 22: 252-259
Pubmed: Author and Title
Google Scholar: Author Only Title Only Author and Title

Ma W, Kong Q, Arondel V, Kilaru A, Bates PD, Thrower NA, Benning C, Ohlrogge JB (2013) WRINKLED1, A Ubiquitous Regulator in Oil Accumulating Tissues from Arabidopsis Embryos to Oil Palm Mesocarp. PLoS ONE 8: e68887
Pubmed: Author and Title
Google Scholar: Author Only Title Only Author and Title

Maatta S, Scheu B, Roth MR, Tamura P, Li M, Williams TD, Wang X, Welti R (2012) Levels of Arabidopsis thaliana leaf phosphatidic acids, phosphatidylserines, and most trienoate-containing polar lipid molecular species increase during the dark period of the diurnal cycle. Frontiers in Plant Science 3: 49
Pubmed: Author and Title
Google Scholar: Author Only Title Only Author and Title

Maréchal E, Bastien O (2014) Modeling of regulatory loops controlling galactolipid biosynthesis in the inner envelope membrane of chloroplasts. Journal of Theoretical Biology 361: 1-13
Pubmed: Author and Title
Google Scholar: Author Only Title Only Author and Title

Meï C, Michaud M, Cussac M, Albrieux C, Gros V, Maréchal E, Block MA, Jouhet J, Rébeillé F (2015) Levels of polyunsaturated fatty acids correlate with growth rate in plant cell cultures. Scientific reports 5: 15207
Pubmed: Author and Title
Google Scholar: Author Only Title Only Author and Title

Miquel M, James D, Dooner H, Browse J (1993) Arabidopsis requires polyunsaturated lipids for low-temperature survival. Proceedings of the National Academy of Sciences 90: 6208-6212
Pubmed: Author and Title
Google Scholar: Author Only Title Only Author and Title

Moellering ER, Muthan B, Benning C (2010) Freezing Tolerance in Plants Requires Lipid Remodeling at the Outer Chloroplast

Membrane. Science 330: 226-228
Pubmed: Author and Title
Google Scholar: Author Only Title Only Author and Title

Mongrand S, Bessoule JJ, Cabantous F, Cassagne C (1998) The C-16 : 3/C-18 : 3 fatty acid balance in photosynthetic tissues from 468 plant species. Phytochemistry 49: 1049-1064
Pubmed: Author and Title
Google Scholar: Author Only Title Only Author and Title

Narayanan S, Tamura PJ, Roth MR, Prasad PVV, Welti R (2016) Wheat leaf lipids during heat stress: I. High day and night temperatures result in major lipid alterations. Plant, Cell & Environment 39: 787-803
Pubmed: Author and Title
Google Scholar: Author Only Title Only Author and Title

Ohlrogge J, Browse J (1995) Lipid Biosynthesis. Plant Cell 7: 957-970
Pubmed: Author and Title
Google Scholar: Author Only Title Only Author and Title

Pham A-T, Lee J-D, Shannon JG, Bilyeu KD (2010) Mutant alleles of FAD2-1A and FAD2-1Bcombine to produce soybeans with the high oleic acid seed oil trait. BMC Plant Biology 10: 195
Pubmed: Author and Title
Google Scholar: Author Only Title Only Author and Title

Rahman MM, Divi UK, Liu Q, Zhou X, Surinder S, Aruna K (2016) Oil-rich nonseed tissues for enhancing plant oil production. CAB Reviews 11: 1-11
Pubmed: Author and Title
Google Scholar: Author Only Title Only Author and Title

Roughan PG, Slack CR (1982) Cellular-organization of glycerolipid metabolism. Annual Review of Plant Physiology and Plant Molecular Biology 33: 97-132
Pubmed: Author and Title
Google Scholar: Author Only Title Only Author and Title

Sakaki T, Saito K, Kawaguchi A, Kondo N, Yamada M (1990) Conversion of Monogalactosyldiacylglycerols to Triacylglycerols in Ozone-Fumigated Spinach Leaves. Plant Physiology 94: 766-772
Pubmed: Author and Title
Google Scholar: Author Only Title Only Author and Title

Schwender J, König C, Klapperstück M, Heinzel N, Munz E, Hebbelmann I, Hay JO, Denolf P, De Bodt S, Redestig H, Caestecker E, Jakob PM, Borisjuk L, Rolletschek H (2014) Transcript abundance on its own cannot be used to infer fluxes in central metabolism. Frontiers in Plant Science 5: 668
Pubmed: Author and Title
Google Scholar: Author Only Title Only Author and Title

Slack CR, Bertaud WS, Shaw BD, Holland R, Browse J, Wright H (1980) Some studies on the composition and surface properties of oil bodies from the seed cotyledons of safflower (Carthamus tinctorius) and linseed (Linum ustatissimum). Biochemical Journal 190: 551-561
Pubmed: Author and Title
Google Scholar: Author Only Title Only Author and Title

Slack CR, Roughan PG, Balasingham N (1977) Labeling studies in vivo on metabolism of acyl and glycerol moieties of glycerolipids in developing maize leaf. Biochemical Journal 162: 289-296
Pubmed: Author and Title
Google Scholar: Author Only Title Only Author and Title

Sperling P, Heinz E (1993) Isomeric sn-1-octadecenyl and sn-2-octadecenyl analogs of lysophosphatidylcholine as substrates for acylation and desaturation by plant microsomal-membranes. European Journal of Biochemistry 213: 965-971
Pubmed: Author and Title
Google Scholar: Author Only Title Only Author and Title

Sperling P, Linscheid M, Stocker S, Muhlbach HP, Heinz E (1993) In-vivo desaturation of cis-delta-9-monounsaturated to cis-delta-9,12-diunsaturated alkenylether glycerolipids. Journal of Biological Chemistry 268: 26935-26940
Pubmed: Author and Title
Google Scholar: Author Only Title Only Author and Title

Stymne S, Stobart AK (1984) THE BIOSYNTHESIS OF TRIACYLGLYCEROLS IN MICROSOMAL PREPARATIONS OF DEVELOPING COTYLEDONS OF SUNFLOWER (HELIANTHUS-ANNUUS L). Biochemical Journal 220: 481-488
Pubmed: Author and Title
Google Scholar: Author Only Title Only Author and Title

Tjellström H, Yang Z, Allen DK, Ohlrogge JB (2012) Rapid Kinetic Labeling of Arabidopsis Cell Suspension Cultures: Implications for Models of Lipid Export from Plastids. Plant Physiology 158: 601-611
Pubmed: Author and Title
Google Scholar: Author Only Title Only Author and Title

Vanhercke T, Divi UK, El Tahchy A, Liu Q, Mitchell M, Taylor MC, Eastmond PJ, Bryant F, Mechanicos A, Blundell C, Zhi Y, Belide S, Shrestha P, Zhou XR, Ral JP, White RG, Green A, Singh SP, Petrie JR (2017) Step changes in leaf oil accumulation via iterative metabolic engineering. Metab Eng 39: 237-246
Pubmed: Author and Title
Google Scholar: Author Only Title Only Author and Title

Vanhercke T, Dyer JM, Mullen RT, Kilaru A, Rahman MM, Petrie JR, Green AG, Yurchenko O, Singh SP (2019) Metabolic engineering for enhanced oil in biomass. Progress in Lipid Research 74: 103-129
Pubmed: Author and Title
Google Scholar: Author Only Title Only Author and Title

Vanhercke T, El Tahchy A, Liu Q, Zhou X-R, Shrestha P, Divi UK, Ral J-P, Mansour MP, Nichols PD, James CN, Horn PJ, Chapman KD, Beaudoin F, Ruiz-López N, Larkin PJ, de Feyter RC, Singh SP, Petrie JR (2014) Metabolic engineering of biomass for high energy density: oilseed-like triacylglycerol yields from plant leaves. Plant Biotechnology Journal 12: 231-239
Pubmed: Author and Title
Google Scholar: Author Only Title Only Author and Title

Vogel C, Marcotte EM (2012) Insights into the regulation of protein abundance from proteomic and transcriptomic analyses. Nature reviews genetics 13: 227
Pubmed: Author and Title
Google Scholar: Author Only Title Only Author and Title

Wang L, Shen W, Kazachkov M, Chen G, Chen Q, Carlsson AS, Stymne S, Weselake RJ, Zou J (2012) Metabolic Interactions between the Lands Cycle and the Kennedy Pathway of Glycerolipid Synthesis in Arabidopsis Developing Seeds. The Plant Cell Online 24: 4652-4669
Pubmed: Author and Title
Google Scholar: Author Only Title Only Author and Title

Williams JP, Imperial V, Khan MU, Hodson JN (2000) The role of phosphatidylcholine in fatty acid exchange and desaturation in Brassica napus L. leaves. Biochemical Journal 349: 127-133
Pubmed: Author and Title
Google Scholar: Author Only Title Only Author and Title

Wood CC, Okada S, Taylor MC, Menon A, Mathew A, Cullerne D, Stephen SJ, Allen RS, Zhou XR, Liu Q (2018) Seed-specific RNAi in safflower generates a superhigh oleic oil with extended oxidative stability. Plant biotechnology journal 16: 1788-1796
Pubmed: Author and Title
Google Scholar: Author Only Title Only Author and Title

Xu C, Shanklin J (2016) Triacylglycerol Metabolism, Function, and Accumulation in Plant Vegetative Tissues. Annual Review of Plant Biology 67: 179-206
Pubmed: Author and Title
Google Scholar: Author Only Title Only Author and Title

Yamauchi R, Kojima M, Isogai M, Kato K, Ueno Y (1982) Separation and Purification of Molecular Species of Galactolipids by High Performance Liquid Chromatography. Agricultural and Biological Chemistry 46: 2847-2849
Pubmed: Author and Title
Google Scholar: Author Only Title Only Author and Title

Yang W, Wang G, Li J, Bates PD, Wang X, Allen DK (2017) Phospholipase Dzeta Enhances Diacylglycerol Flux into Triacylglycerol. Plant Physiol 174: 110-123
Pubmed: Author and Title
Google Scholar: Author Only Title Only Author and Title

Zhou XR, Shrestha P, Yin F, Petrie JR, Singh SP (2013) AtDGAT2 is a functional acyl-CoA:diacylglycerol acyltransferase and displays different acyl-CoA substrate preferences than AtDGAT1. FEBS Lett 587: 2371-2376
Pubmed: Author and Title
Google Scholar: Author Only Title Only Author and Title

Zou JT, Wei YD, Jako C, Kumar A, Selvaraj G, Taylor DC (1999) The Arabidopsis thaliana TAG1 mutant has a mutation in a diacylglycerol acyltransferase gene. Plant Journal 19: 645-653
Pubmed: Author and Title
Google Scholar: Author Only Title Only Author and Title